Climate Dynamics
https://doi.org/10.1007/s00382-020-05486-x

Changes in extended boreal summer tropical cyclogenesis associated with large-scale flow patterns over the western North Pacific in response to the global warming hiatus

Kai Zhao[1] · Haikun Zhao[2,3] · Graciela B. Raga[4] · Ryuji Yoshida[5,6,7,8] · Weiqiang Wang[3,9,10] · Philip J. Klotzbach[11]

Received: 10 February 2020 / Accepted: 3 October 2020

Abstract
This study examines extended boreal summer (May–October) tropical cyclogenesis events (TCGEs) associated with large-scale flow patterns (LFPs) over the western North Pacific (WNP) between 1979–1997 and 1998–2012. WNP TCGEs are objectively identified to be associated with five LFPs [e.g., monsoon shear line (SL), monsoon confluence region (CR), monsoon gyre (GY), Pacific easterly wave (EW) and preexisting tropical cyclone (PTC)]. Results show that an apparent decrease in TCGEs from 1998–2012 was due to the significant decrease in TCGEs associated with the PTC pattern and to a somewhat lesser degree, TCGEs associated with the GY pattern. In contrast, TCGEs associated with the SL pattern show a small increase, which seems to contradict the weakened monsoon circulation since 1998 but corresponds well to cyclonic anomalies over the Philippines region. Decreased TCGEs associated with the GY pattern and increased TCGEs associated with the EW pattern are closely related to the strengthening of Pacific easterly waves in response to the Mega La Niña-like pattern that predominated during 1998–2012. Weakened easterly shear over the eastern WNP is not conducive to the development and propagation into the southeastern WNP of Rossby wave trains induced by preexisting TC energy dispersion. Consequently, there is a significant reduction of TCGEs associated with the PTC pattern and a weakening in the contribution of TCGEs associated with the PTC pattern to TCGEs associated with the EW pattern. An increased correlation between TCs associated with the SL/GY/EW patterns and central Pacific (CP)-type ENSO during 1998–2012 is observed. A stable and robust association between TCGEs associated with the CR pattern and tropical North Atlantic sea surface temperature is observed regardless of decadal climate regime shifts. However, there is no significant link between TCGEs associated with the PTC pattern and more CP ENSO events during 1998–2012, but there is a strong association between the Pacific meridional mode and TCGEs associated with the PTC pattern during 1979–1997. More observational analyses and numerical simulations are needed to further investigate the underlying physical mechanism.

Keywords Large-scale flow pattern · Tropical cyclogenesis · Western North Pacific · Mega la Niña-like pattern · Global warming hiatus

1 Introduction

The western North Pacific (WNP) is the most active TC basin for tropical cyclogenesis (TCG) around the world on an annually-averaged basis (Schreck et al. 2014). About one-third of global tropical cyclones (TCs) occur annually over the WNP (Chan 2005; Schreck et al. 2014), which can cause tremendous loss of life and property to the coastal regions of East Asia (Zhang et al. 2009, 2011). Some studies have suggested that global warming may cause more TCs tracking northwestward over the WNP basin (Wu and Wang 2004; Wang and Wu 2015) and thus, posing an increased threat to East Asia (Oouchi et al. 2006; Bengtsson et al. 2007; Knutson et al. 2010). Improved understanding of WNP TC activity at various time scales in response to climate change is therefore of great scientific significance and socio-economic interest.

Several studies have suggested that WNP TCG events (TCGEs) undergoes remarkable inter-decadal changes due to inter-decadal changes in the large-scale atmospheric and oceanic environment (Yumoto and Matsuura 2001;

✉ Haikun Zhao
zhk2004y@gmail.com

Extended author information available on the last page of the article

Published online: 13 October 2020

Matsuura et al. 2003; Chan 2008; Liu and Chan 2008, 2013; Hong et al. 2016; Zhao et al. 2018, 2019b). The significant decrease in TCGEs over the WNP basin from ~ 1998 to 2012 has been discussed extensively in the literature (Liu and Chan 2013; Yokoi and Takayabu 2013; He et al. 2015; Choi et al. 2016a, b). This inter-decadal change in TCGEs was likely closely associated with the transition of the Pacific Decadal Oscillation (PDO) phase from warm to cold and a shift in El Niño-Southern Oscillation (ENSO) characteristics to more frequent central Pacific (CP)-type ENSO events (Verdon and Franks 2006; Kao and Yu 2009; Yu et al. 2015). Associated with these changes, it has been a westward shift of the monsoon trough and the tropical upper-tropospheric trough (TUTT) (Zhao et al. 2019a, b; Wu et al. 2015). This leads to enhanced vertical wind shear and reduced low-level vorticity, especially over the southeastern portion of the WNP basin (Wang and Wu 2016; Hu et al. 2018; Zhao et al. 2019a, b), which agrees well with a significant decrease in TCG over the WNP basin from ~ 1998 to 2012 (Maue 2011; Liu and Chan 2013; Hsu et al. 2014; Hu et al. 2018; Zhao et al. 2019a, b).

Changes in TCG are generally controlled by changes in large-scale dynamic and thermodynamic conditions, with warm sea surface temperature (SST), weak vertical wind shear, high low-level vorticity, and mid-level relative humidity all considered favorable for TCG (Gray 1968, 1979, 1998; McBride and Zehr 1981; Jiang et al. 2012) and these changes in the environmental factors affecting TCGEs are generally associated with changes in the large-scale circulation. Therefore, a better understanding of TCGEs associated with large-scale flow patterns (LFPs) would be useful both for prediction and for an improved understanding of the underlying physical mechanisms. Several studies have identified and classified LFPs favorable for TCGs (Zehr 1992; Ritchie and Holland 1999; Lee et al. 2008). Zehr (1992) investigated the environmental flow for TCGEs related to the monsoon trough over the WNP basin and identified three LFPs: strong westerly, weak westerly and strong easterly. Subsequently, Ritchie and Holland (1999, hereafter RH99) further classified the LFPs for TCGEs into five basic LFPs: monsoon shear line (SL), monsoon confluence region (CR), monsoon gyre (GY), easterly wave (EW), and Rossby wave energy dispersion. However, the classification of LFPs for TCGEs in these prior studies was subjective and consequently, it makes it challenging to reproduce their associated results.

Yoshida and Ishikawa (2013) proposed an objective classification approach to classify environmental flows into the five LFPs as identified by RH99: SL, CR, GY, EW, and pre-existing TC (PTC) (the PTC pattern is similar to the pattern associated with Rossby wave energy dispersion in RH99). They further noted that the results based upon this objective classification were almost identical to the results of RH99. Using this objective method, Zhao et al. (2015, 2016) subsequently investigated the distinct impact of the boreal summer intra-seasonal oscillation including the Madden–Julian oscillation (MJO) and quasi-biweekly oscillation (QBWO) on TCG associated with these five LFPs. There is a significant inter-decadal change in TC frequency over the WNP basin (Zhao et al. 2016, 2018; Hu et al. 2018) as well as in relationships between inter-annual teleconnections and TCGEs (Choi et al. 2019; Zhao et al. 2019a, b). For example, Zhao et al. (2019a) found a recent strengthening of the inter-annual relationship between the monsoon trough and TC frequency over the WNP basin. A few studies have found a warm shift in the Pacific and global temperatures rise sharply during 1979–1997, while the warming stalled and the eastern Pacific flipped into a cool sate during 1998–2012 that was called "global warming hiatus" (Kosaka and Xie 2013; Fyfe et al. 2013; Tollefson 2014). The tropical central Pacific exhibits a relatively large cool SSTA pattern during 1998–2012 in agreement with on the PDO phase change (Liu and Chan 2008, 2013; Zhao and Wang 2016, 2019) and an increasing occurrence of La Niña and Central Pacific El Niño events during 1998–2012 (Ashok et al. 2007; Yu and Kao 2007; Kug et al. 2009; Lee and McPhaden 2010; Hu et al. 2018; Zhao and Wang 2019). A question naturally arises: How do TCGEs associated with each of the five basic LFPs contribute to the substantial decrease in TCGEs over the WNP basin during the "global warming hiatus" period of 1998–2012?

The rest of this study is organized as follows. Section 2 describes the data and methodology used. Section 3 investigates the contributions of changes in TCGEs associated with each of the five LFPs to the overall decrease in TCGEs over the WNP basin between 1979–1997 (the accelerated warming period) and 1998–2012 (global warming hiatus period). Section 4 explores the possible associated physical mechanisms for the observed inter-decadal changes in TCGEs associated with each of the five basic LFPs. Section 5 presents a discussion and provides some conclusions.

2 Data and methodology

2.1 TC data, atmospheric and oceanic datasets

The TC data from 1979 to 2012 is obtained from the best-track dataset of the Joint Typhoon Warning Center (JTWC) (Chu et al. 2002). This data includes TC latitude and longitude, maximum sustained surface winds and minimum sea level pressure (since 2001 for most TCs) at a 6-h interval. In contrast to prior studies focused on TCs with an intensity greater than or equal to 34 kt (i.e., at least tropical storm intensity), this study primarily focuses on the early stage of TCG and, therefore, all TCGEs with an intensity greater

than or equal to 20 kt are considered. The TCG location is defined as the first location where the intensity of the TC reaches 20 kt. All TCGEs during the peak TC season from May to October over the WNP basin [0–30° N, 100–180° E] are analyzed in this study.

The atmospheric fields are archived from the NCEP/DOE AMIP-II Reanalysis (Reanalysis-2), with a horizontal resolution of 2.5° × 2.5° and 17 vertical pressure levels (Kanamitsu et al. 2002). Monthly sea surface temperature (SST) are obtained from the extended reconstructed SST version 5 (ERSSTv5) from NOAA that provides global, spatially complete SST data for the period 1854–present, with a latitudinal and longitudinal horizontal resolution of 2.0° × 2.0° (Huang et al. 2017). The 6-hourly variables including winds, relative humidity, temperature and SST derived from the JRA-25/JMA Climate Data Assimilation System (Onogi et al. 2007) are used to objectively identify the five basic LFPs favorable for TCGEs over the WNP basin during the peak TC season from May to October.

To analyze the relationship between large-scale ocean-atmospheric conditions and TCGEs associated with the identified five basic LFPs, several climate indices, including the Pacific Decadal Oscillation (PDO) and ENSO, are used. The PDO index is the leading principal components of monthly SST anomalies in the North Pacific Ocean (Mantua et al. 1997). Here we use the PDO as defined by the University of Washington: https://research.jisao.washington.edu/pdo/PDO.latest.txt. As suggested by previous studies, due to shifts in ENSO characteristics (Ashok et al. 2007; Yu et al. 2011), two ENSO indices: the El Niño Modoki index (EMI) and the Niño-3.4 index, are adopted. The Niño-3.4 index is defined as SST anomalies (SSTAs) over the region [5° S–5° N, 170°–120° W], which generally represents the traditional ENSO state. The EMI index was proposed to represent CP ENSO events (Ashok et al. 2007) and has been widely used in many prior studies (Ashok et al. 2007; Zhao and Wang 2019; Zhao et al. 2019a). Following Ashok et al. (2007), the EMI index is calculated with the following expression (1):

$$\begin{aligned} \mathrm{EMI} = {} & [\mathrm{SSTA}]_{[165^\circ\,\mathrm{E}-140^\circ\,\mathrm{W},10^\circ\,\mathrm{S}-10^\circ\,\mathrm{N}]} - 0.5 \\ & \times [\mathrm{SSTA}]_{[125^\circ\,\mathrm{E}-145^\circ\mathrm{E},10^\circ\,\mathrm{S}-20^\circ\,\mathrm{N}]} - 0.5 \\ & \times [\mathrm{SSTA}]_{[110^\circ\,\mathrm{W}-70^\circ\,\mathrm{W},15^\circ\,\mathrm{S}-5^\circ\,\mathrm{N}]} \end{aligned} \quad (1)$$

2.2 Classification of TCGEs associated with the five basic LFPs

Following Yoshida and Ishikawa (2013), the LFPs associated with the 793 TCGEs over the WNP basin during May–October from 1979 to 2012 are classified. In this objective classification method, the LFP with the largest normalized contribution score is identified as the flow pattern for each TCGE. The contribution score for each of the SL, CR, GY and EW flow patterns is largely associated with the 850-hPa averaged wind field before a TCGE. The contribution of the PTC pattern is primarily scored by the minimum sea level pressure of a TCGE and the detected obvious wave train at the time of a TCGE. Details on the computational methodology for the normalized contribution score can be found in Yoshida and Ishikawa (2013).

Figure 1 gives typical examples of TCGEs corresponding to the five basic LFPs. The case displayed in Fig. 1a shows a highest contribution score from the SL flow pattern, with a weak contribution score from the PTC pattern. Therefore, the SL flow pattern is identified with this TCGE. Similarly, the CR flow pattern is identified as the major contribution pattern to the TCGE displayed in Fig. 1b. Figure 1c presents a TCGE where the contribution score is largest from the GY pattern, with a secondary contribution from the SL pattern. Figure 1d shows a TCGE where the EW pattern predominates, while the PTC pattern is the major contribution pattern to TCGE in the case displayed in Fig. 1e, where a preexisting TC already existed. Additionally, an unclassified flow pattern is displayed in Fig. 1f, where no distinct scores are achieved for any of the five flow patterns of interest.

The 793 WNP TCG cases associated with the five basic LFPs are classified as follows: 317 (40%) SL-associated, 153 (19%) CR-associated, 126 (16%) EW-associated, 96 (12%) PTC-associated, and 45 (6%) GY-associated. These results are consistent with previous studies on the critical importance of the monsoon circulation over the WNP basin (Ritchie and Holland 1999; Molinari and Vollaro 2013; Yoshida and Ishikawa 2013; Zhao et al. 2015, 2016), with ~ 65% of the total number of TCGEs being associated with the monsoon-related flow patterns represented by SL, CR and GY. There are some slight differences in the percentage of TCGEs associated with the LFPs between this study and previous studies (Ritchie and Holland 1999; Yoshida and Ishikawa 2013; Zhao et al. 2015, 2016). These discrepancies may be due to different detection algorithms, different study periods as well as different datasets. Additionally, 56 (7%) of the TCGEs investigated in this study belong to the unclassified large-scale pattern. We recommend that these TCGEs be investigated in more detail in future work.

2.3 Statistical significance test

The one-tailed *Student t-test* is used to determine the statistical significance of the composite difference and correlation coefficients in this study. A *P-value* less than or equal to 0.10 is deemed to be significant, unless specifically stated otherwise in this study.

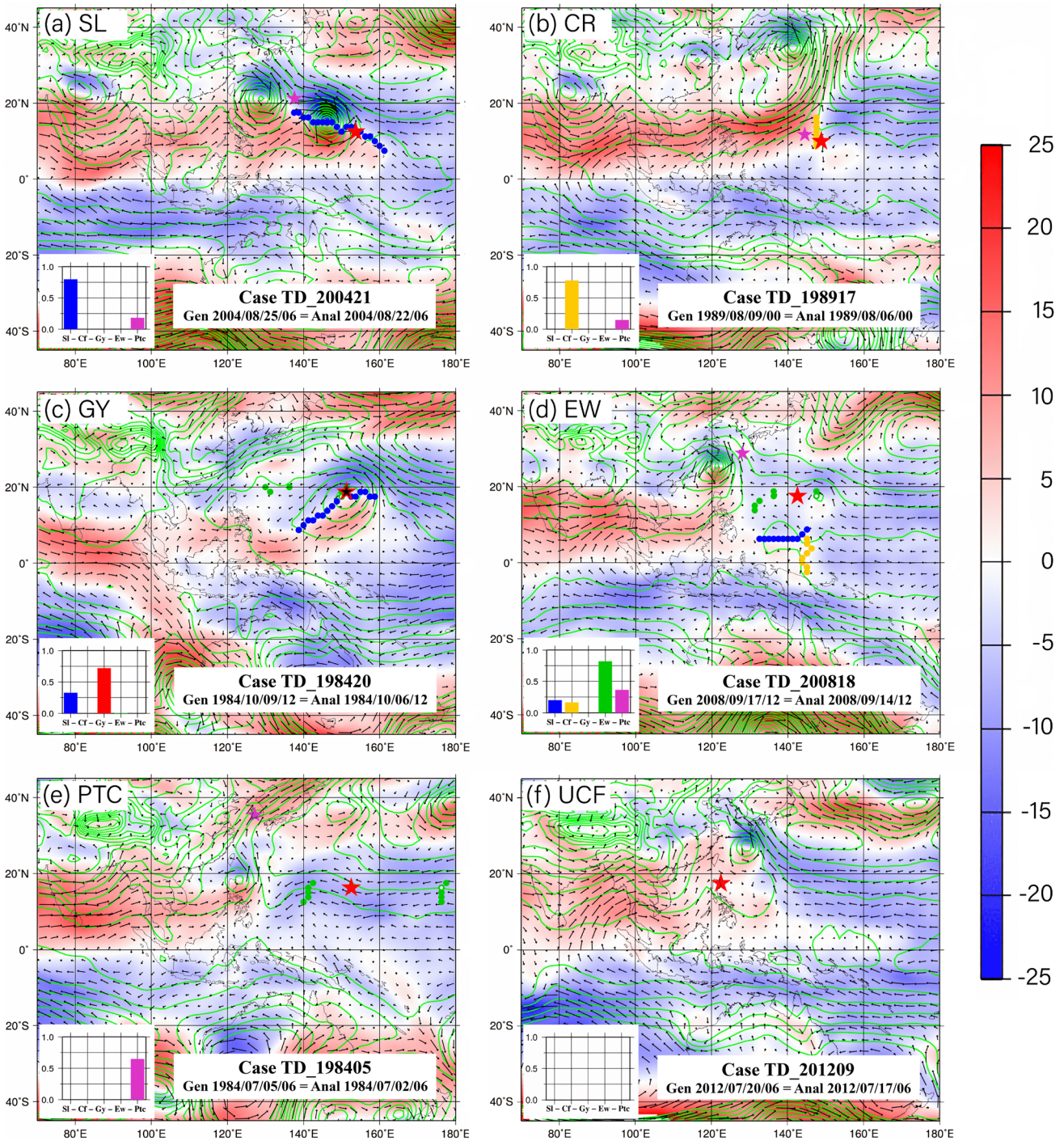

Fig. 1 Typical cases of flow patterns: **a** SL, **b** CR, **c** GY, **d** EW, **e** PTC, and **f** Unclassified (UCF). Sea level pressure (contours) and 850-hPa wind (vector) are also displayed. The red star represents the TCG location, and the purple star represents PTC. Blue dots denote the shear line, while yellow dots denote the confluence region, and green dots denote an easterly wave. The contribution score of each of the five flow patterns are listed in the inset. The shading indicates the value in the 850 hPa zonal wind speed

3 Interdecadal and inter-annual change of TCGEs associated with LFPs

3.1 Interdecadal change of TCGEs associated with LFPs

An average of 23.2 TCs occurred during May–October over the WNP basin for the period 1979–2012 with a standard deviation (STD) of 4.2 TCs, indicating strong inter-annual variability in TC counts. Each of the five LFPs also show considerable interannual variability in terms of the number of TCs that they generate, with a STD of 3.2 TCs for the SL pattern, 2.6 TCs for the CR pattern, 1.3 TCs for the GY pattern, 1.9 TCs for the EW pattern, and 2.5 TCs for the PTC pattern, respectively.

There was a significant decrease in both TCGEs as well as the STD from 23.4 ± 4.6 in (1979–1997) to 22.0 ± 3.5 in (1998–2012) over the WNP basin, consistent with previous studies (Liu and Chan 2013; Hu et al. 2018; Zhao et al. 2019a). This weakened inter-annual variability in the number of WNP TCGEs since 1998 may be closely associated with the weakened variance in the tropical Pacific sea surface temperature (SST) since the late-1990s (Hu et al. 2013, 2018). To further understand the decrease in TCGEs over the WNP basin from changes in the number of TC formations associated with the five basic LFPs, the difference in TC counts associated with each of the five large-scale patterns is examined between 1979–1997 and 1998–2012 (Table 1). There has been a moderate increase of 1.1 TCs per year associated with the SL pattern from 1979–1997 to 1998–2012, which is in opposition to the observed decrease in the total TCGEs over the WNP basin during the later period. In contrast, there has been a moderate decrease in TCGEs associated with the CR pattern and a significant decrease in TCGEs associated with the GY pattern during the later period. When considering all TCGEs associated with the large-scale pattern related to the monsoon (i.e., SL, CR and GY patterns), a small increase in the number of monsoon-related TCGEs is found, which appears to be inconsistent with results from previous studies on the westward shift of the monsoon circulation over the WNP basin (Hsu et al. 2014; Lin and Chan 2015; Zhao et al. 2019b). In this sense, the extension of the monsoon trough over the WNP basin has a significant impact on the TC formation location but no apparent impact on the total number of TCs associated with the monsoon trough (Lander 1994; Wang and Chan 2002; Zhao et al. 2010). The annually-averaged TC count associated with the PTC pattern decreased from 3.8 (1979–1997) to 1.6 (1998–2012), with also a reduced STD from 2.8 to 1.3 (Table 1). The difference in the annual average of TCGEs associated with the PTC pattern is 2.2, accounting for ~ 66% of the observed total reduction of WNP TCGEs found during the later period. In addition, a weak decrease in TC counts associated with the EW pattern is also found during 1998–2012.

The difference of the total TCs between the two epochs shows a dipole distribution, as seen in Fig. 2. The WNP is further divided into four sub-regions to investigate the regional difference of TC genesis for different large-scale flow pattern: northwestern sub-region: 110°–140° E, 15°–25° N; northeastern sub-region: 140°–180° E, 15°–25° N; southwestern sub-region: 110°–140° E, 5°–15° N, and southeastern sub-region: 140°–180° E, 5°–15° N. Results show that the decrease of WNP TC counts during 1998–2012 is primarily due to a significant reduction in TCs over the southeastern sub-region of WNP basin (Table 2), where TC counts decreased from 9.1 TCs (1979–1997) to 4.4 TCs (1998–2012) on average. Moreover, Table 2 indicates that each of the five LFPs also shows a significant reduction in the annual average of TC counts over the southeastern sub-region of WNP basin during the global warming hiatus period compared to the accelerated warming period, with a decrease of 1.3 TCs for the SL pattern, 0.9 TCs for the CR pattern, 0.6 TCs for the GY pattern, 0.8 TCs for the EW pattern, and 1.2 TCs for the PTC pattern, respectively. In particular, there are no TCs associated with the GY pattern over the

Table 1 Annually-averaged TC frequency/latitude/longitude for all TCs over the WNP basin and associated with the SL, CR, GY, EW, and PTC patterns, respectively during the first sub-period 1979–1997 (P1) and the second sub-period 1998–2012 (P2), and their differences (1998–2012 minus 1979–1997)

	Frequency P1/P2/P2 – P1	Latitude P1/P2/P2 – P1	Longitude P1/P2/P2 – P1
Total	24.3/22.0/**– 2.25****	13.45/15.45/**2.0****	144.70/138.17/**– 6.53****
SL	8.84/9.93/1.09	12.83/14.98/**2.15****	143.05/135.93/**– 7.12****
CR	4.53/4.47/– 0.06	13.97/14.78/0.81	140.23/138.94/– 1.29
GY	1.68/0.87/**– 0.81****	13.45/15.39/1.94	141.76/130.74/**– 11.02****
EW	3.74/3.67/– 0.07	13.56/16.57/**3.01****	148.14/140.75/**– 7.39****
PTC	3.79/1.6/**– 2.19****	12.57/16.81/**4.24****	154.83/151.03/– 3.80
UCF	1.74/1.53/– 0.20	16.95/16.31/– 0.64	138.12/135.04/– 3.08

The unclassified flow (UCF) pattern are determined by no distinct scores achieved for any of the five flow patterns of interest. The symbol "**" indicates that the differences are significant at a 90% confidence level

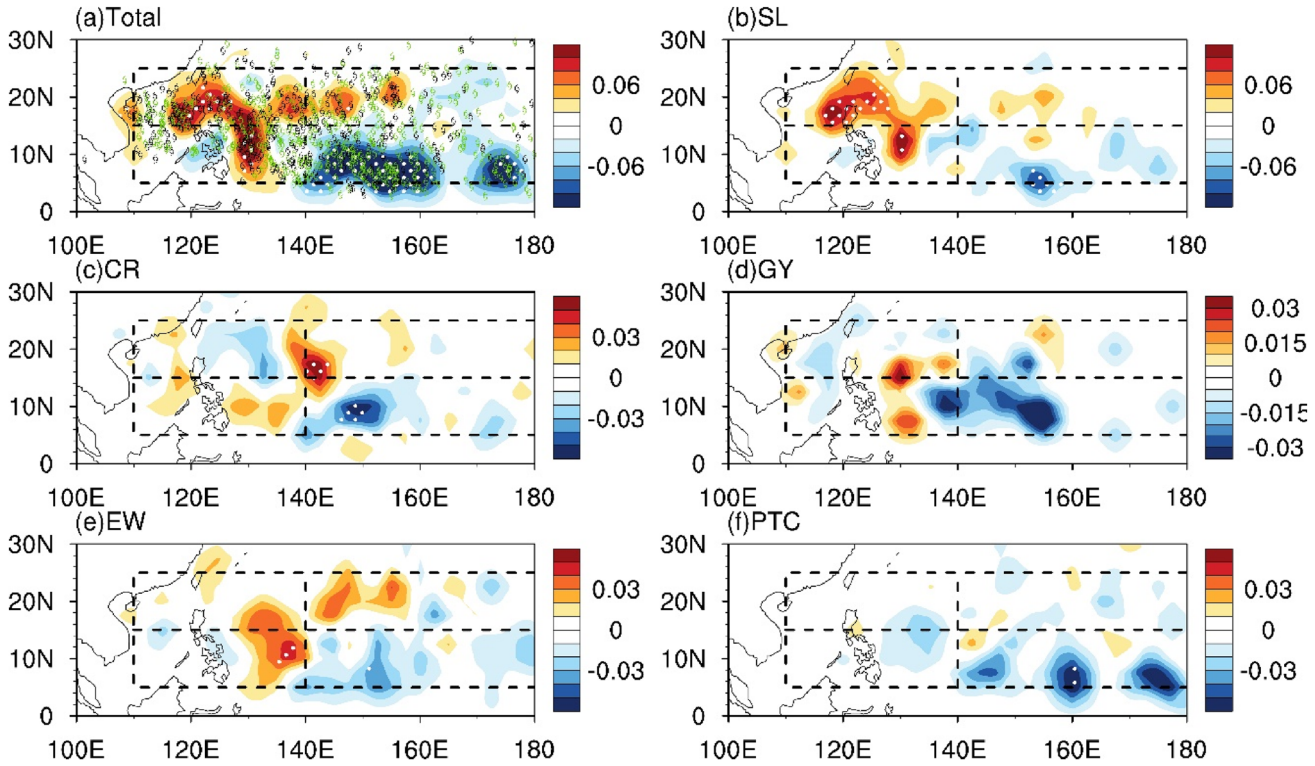

Fig. 2 Spatial distribution of the difference in the total TC count between 1979–1997 and 1998–2012 (i.e., 1998–2012 minus 1979–1997) for **a** the total number of TCs, **b** TCs associated with the SL pattern, **c** TCs associated with the CR pattern, **d** TCs associated with the GY pattern, **e** TCs associated with the EW pattern and **f** TCs associated with the PTC pattern. The areas with white dots indicate that the differences are significant at a 90% confidence level. The sub-regions are also show in figure: northwestern (110–140° E, 15–25° N), northeastern (140–180° E, 15–25° N), southwestern (110–140° E, 5–15° N), and southeastern region (140–180° E, 5–15° N). The TCG locations are marked with green symbol during 1979–1997, and black symbol during 1998–2012

Table 2 Annually-averaged TC frequency for all TCs over the northwestern, northeastern, southwestern, and southeastern sub-regions of the WNP basin and associated with the SL, CR, GY, EW, and PTC patterns, respectively during the first sub-period 1979–1997 (P1) and the second sub-period 1998–2012 (P2), and their differences (1998–2012 minus 1979–1997)

	NW P1/P2/P2 – P1	NE P1/P2/P2 – P1	SW P1/P2/P2 – P1	SE P1/P2/P2 – P1
Total	4.26/6.73/**2.47****	4.00/3.93/−0.07	5.05/5.40/0.35	9.16/4.47/−**4.69****
SL	1.47/3.27/**1.80****	1.37/1.40/0.03	2.05/2.60/0.55	3.37/2.07/−**1.30***
CR	1.16/1.27/0.11	0.53/1.00/0.47	0.95/1.20/0.25	1.74/0.80/−**0.94***
GY	0.32/0.33/0.01	0.32/0.13/−0.18	0.42/0.40/−0.02	0.63/0/−0.63
EW	0.68/0.93/0.25	0.58/1.00/0.42	0.53/0.73/0.21	1.47/0.67/−**0.80****
PTC	0.16/0.27/0.11	0.89/0.40/−0.49	0.53/0.13/−**0.40***	1.84/0.60/−**1.24****

The symbol "*/**" indicates that the differences are significant at a 90/95% confidence level

southeastern sub-region of WNP basin. In contrast, a significant increase of 2.4 TCs is found over the northwestern part of the WNP, which is primarily due to a significant increase of 1.7 TCs associated with the SL pattern. The differences in TCs associated with the other four patterns between 1979–1997 and 1998–2012 are not significant over the northwestern sub-region of WNP basin. Over the northeastern or southwestern sub-regions, there is no significant change in TC counts during the two periods. However, the TCGEs associated with the PTC pattern has a significant decrease of 0.40 TCs (from 0.53 during 1979–1997 to 0.13 during 1998–2012) over the southwestern sub-region. A moderate increase in TCs associated with the CR or EW patterns is found over the southwestern, northeastern, and northwestern sub-regions, which

largely offset the significant decrease of TCGEs over the southeastern sub-region.

In summary, the decrease in WNP TC counts during 1998–2012 is primarily due to a significant reduction in TCGEs associated with the PTC pattern with a secondary contribution from the TCGEs associated with the GY pattern. In terms of PTC cases associated with a newly-generated low-pressure area modulated by a pre-existing mature TC, the thermodynamic and dynamic conditions are not suitable, and consequently, the disturbance cannot develop into a TC as would be expected. In agreement with previous studies on the westward shift of the large-scale circulation (Wu et al. 2015; Wu and Wang 2015; Wang and Wu 2016; Hu et al. 2018; Zhao et al. 2019a, b), the annual-averaged formation location for all TCs as well as TCs associated with each of the five LFPs show a consistent west-northward shift, although their amplitude exhibits some differences (Table 1 and Fig. 2). In general, there is a significant decrease in TCs over the eastern portion of the WNP basin and an increase in TCs over the western portion of the WNP basin (Fig. 2), with the exception of TCs associated with the PTC large-scale pattern. In this latter case, there is a consistent WNP basin-wide decrease from 1979–1997 to 1998–2012 (Fig. 2).

3.2 Cross inter-annual correlation among the LFPs

As shown in Fig. 3 and Table 3, TCs associated with monsoon-related large-scale patterns (i.e., the SL, CR and GY patterns) significantly correlate with the total TCs (r = 0.51). This implies that the inter-annual change in TCGEs is primarily controlled by changes in the monsoon circulation over the WNP basin, agreeing well with prior studies that noted the importance of the monsoon trough in controlling the inter-annual variability of TCGEs over the WNP basin (Wang and Zhou 2008; Wu et al. 2012; Zong and Wu 2015a, b; Choi et al. 2016a,b; Zhao et al. 2019a, b).

We further examine the inter-annual relationship between the TCs associated with monsoon-related large-scale patterns between the two epochs (Table 3). There is an inter-decadal change in the inter-annual relationship between TCs associated with the SL pattern and the total TCs, with a significant correlation (r = 0.49) during 1979–1997 but insignificant (r = 0.34) during 1998–2012. TCs associated with the CR pattern significantly correlate with total TCs during 1979–1997 (r = 0.40) and 1998–2012 (r = 0.59), while the correlation between TCs associated with the GY pattern and total TCs is not significant during both sub-periods. Together with the reduced frequency associated with the GY pattern compared to that associated with the CR or SL patterns, TCs associated with the GY pattern may have limited influence in the inter-annual changes of the total TCs. In this sense, it seems that the monsoon modulation of TCs is primarily caused by changes in TCs associated with the SL and CR pattern. Though the TCs associated with the SL pattern had an insignificant correlation with the total TCGEs since 1998, they can interact with TCs associated with the CR pattern and thus, control the total TCs.

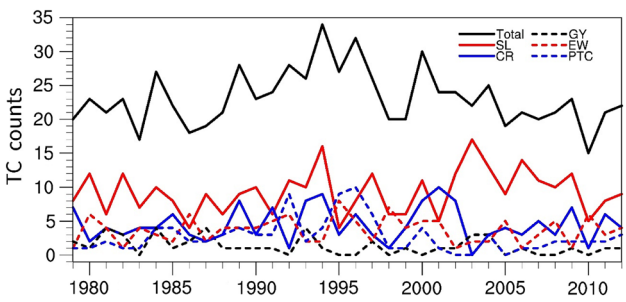

Fig. 3 Time series of total TC counts (black solid line) and TC counts associated with each of the five flow patterns [SL (red solid line), CR (blue solid line), GY (black dotted line), EW (red dotted line) and PTC (blue dotted line)] from 1979 to 2012

Interestingly, there is a significant correlation between TCs associated with the PTC pattern and the total TCs (r = 0.68) (Table 3), agreeing well with previous studies that indicate that an increase in TCGEs possibly enhances its Rossby wave dispersion and consequently, stimulate new TC formation (Li and Fu 2006; Li et al. 2006). Moreover, TCs associated with the PTC pattern can further create a favorable environment for generation of TCs, exerting a relative influence on the inter-annual variability of total TCGEs over the WNP basin. However, TCs associated with the EW pattern do not correlate significantly (r = − 0.02) with the inter-annual change of total TCGEs over the WNP basin (Table 3).

We further investigate the relationship of inter-annual changes in TCs associated with five large-scale patterns and their inter-decadal change. As shown in Table 3, the correlation between TCGEs with the SL pattern and EW pattern is both significant during 1979–1997 (r = − 0.48) and 1998–2012 (r = − 0.78). Such robust and significant association between them is due to the influence on the monsoon circulation, with TCs associated with the SL pattern largely depending on the decreased/enhanced vertical wind shear and TCs associated with the EW pattern largely depending on the weakened/enhanced easterly wind. The correlation between TCGEs and the SL patterns and GY pattern has strengthened from 0.10 (insignificant during 1979–1997) to 0.58 (significant during 1998–2012), and the correlation between TCGEs with the GY pattern and EW pattern is both significant during 1979–1997 (r = − 0.54) and 1998–2012 (r = − 0.57). It seems that the connection between the GY pattern and monsoon circulation strengthened during 1998–2012, similarly to the increased association between TCs associated with SL pattern and EW pattern. However, there is no significant correlation between the

Table 3 Cross-correlation coefficients between TC counts associated with the SL, CR, GY, EW, and PTC patterns, for the first sub-period: 1979–1997(P1), the second sub-period: 1998–2012(P2) and the whole period: 1979–2012(P).

	Total (P/P1/P2)	SL (P/P1/P2)	CR (P/P1/P2)	GY (P/P1/P2)	EW (P/P1/P2)	PTC (P/P1/P2)
Total	/	**0.36****/**0.49****/0.34	**0.45****/**0.40***/**0.59****	−0.02/−0.26/0.24	−0.02/0.09/−0.25	**0.68****/**0.71****/**0.50***
SL	**0.36****/**0.49****/0.34	/	−0.01/0.14/−0.16	0.20/0.10/**0.58****	−**0.61****/−**0.48****/−**0.78****	−0.08/0.008/−0.06
CR	**0.45****/**0.40***/**0.59****	−0.01/0.14/−0.16	/	−0.05/0.002/−0.17	−0.27/−0.36/−0.18	0.02/−0.04/0.19
GY	−0.02/−0.26/0.24	0.20/0.10/**0.58****	−0.05/0.002/−0.17	/	−**0.51****/−**0.54****/−**0.57****	−0.21/−**0.50****/−0.09
EW	−0.02/0.09/−0.25	−**0.61****/−**0.48****/−**0.78****	−0.27/−0.36/−0.18	−**0.51****/−**0.54****/−**0.57****	/	**0.32***/**0.44***/0.16
PTC	**0.68****/**0.71****/**0.50***	−0.08/0.008/−0.06	0.02/−0.04/0.19	−0.21/−**0.50****/−0.09	**0.32***/**0.44***/0.16	/

The symbol "*/**" indicates that the correlation coefficients are significant at a 90/95% confidence level

TCGEs associated with the CR pattern and other patterns. Ritchie and Holland (1999) suggested that the formation of TCs associated with the CR pattern is mainly affected by the monsoon circulation and Pacific easterly waves. There may be nonlinear interactions between the monsoon circulation and tropical Pacific easterly waves, which can influence the generation of TCGEs associated with the CR pattern. The TCGEs associated with the EW and PTC pattern have a significant positive correlation (0.44) during 1979–1997, but the relationship becomes insignificant during 1998–2012 (0.16). The PTC pattern has a great contribution to TCGEs associated with the EW pattern, because the PTC feeds vortices into the easterly wave perturbation to promote TCG. TCGEs associated with the PTC pattern decreased significantly during 1998–2012 and weakened the contribution of the PTC pattern to TCGEs associated with the EW pattern. Similarly, the correlation between the TCGEs associated with the GY and PTC pattern is significant ($r = -0.50$) during 1979–1997, and insignificant ($r = -0.09$) during 1998–2012, which may also relate to vortices feeding on the propagation of Rossby wave energy dispersion in the PTC pattern. In addition, the TCGEs associated with the PTC pattern have no significant correlation with TCGEs associated with the SL and CR pattern.

4 Possible physical mechanism

Changes in the inter-annual variability of TC activity over the WNP basin is closely associated with ENSO, the Atlantic Meridional Mode (AMM), the Pacific Meridional Mode (PMM), trans-basin variability (TBV) and other mechanisms (Du et al. 2011; Zhang et al. 2015, 2016; Choudhury et al. 2017; Wang et al. 2019; Zhao and Wang 2019). However, the inter-decadal changes of TCs associated with each of the five LFPS over the WNP basin remains unclear and will be further investigated in this section from the changes in large-scale environment and relationships with SST.

4.1 Role of changes in the large-scale environment

The difference in SST between the two sub-periods seen in Fig. 4 shows a Mega-La-Niña-like pattern, consistent with previous studies (He et al. 2015; Hong et al. 2016; Zhao et al. 2019a, b). In response to this Mega-La-Niña-like pattern, two large-scale circulations known to significantly impact WNP TC activity (the WNP monsoon trough and the TUTT) have a pronounced westward shift (Fig. 2). An anomalous cyclonic circulation also develops north of the Philippines in the later period (Fig. 4), conducive to TCs over this region and agreeing well with more TCs associated with the SL pattern (Fig. 2b). During 1998–2012, low-level

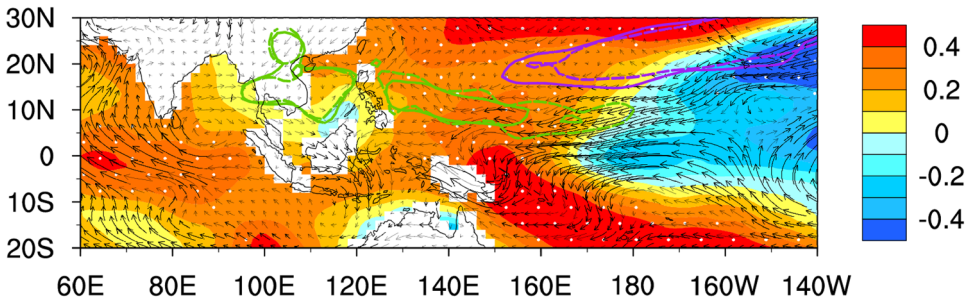

Fig. 4 SST (shading) and 850-hPa wind (vector) difference between 1998–2012 and 1979–1997 (e.g., 1998–2012 minus 1979–1997). The TUTT (purple lines) and WNPMT (green lines) are identified by relative vorticity of 0.3×10^{-5} s^{-1} at 200 hPa and 850 hPa, respectively for 1998–2012 (solid line) and 1979–1997 (dashed line). The white dots and bold black vectors denote that the differences are significant at a 90% confidence level

easterly flow is also strengthened over the tropical southeastern portion of the WNP basin, in partial agreement with an increase of TCs associated with the EW pattern over the WNP basin.

We next investigate differences in vertical wind shear, low-level relative vorticity, and 600-hPa relative humidity between the two sub-periods (Fig. 5). Increased vertical wind shear is found over the main area (110°–180° E, 5°–25° N) where TCs form and especially over the southeastern part of WNP basin, coinciding with a significant decrease in TCs over the southeastern portion of WNP basin. Recall that this study focuses only on TCs with intensity ≥ 20 kt and that more TCs occur at low latitudes and especially over the southeastern region of the WNP basin. Together with change in TC formation locations, an increase in TC counts over the western portion of the WNP basin appears to be contradict with an increase of vertical wind shear, implying a limited role of change in vertical wind shear in modulating TCs over the western portion of WNP basin and other factors should exist. By contrast, a decrease in TC counts over the southeastern portion of the WNP basin corresponds well to a substantial increase of vertical wind shear (Fig. 5), indicating that the intensification of vertical wind shear over the southeastern part of the WNP appears conducive to the decrease of TCG during 1998–2012.

The significant decrease of TCs over both the southeastern and south-central part of WNP basin seen in Fig. 2a is possibly associated with the decreased low-level vorticity (Fig. 5b) in response to a westward shift of the WNP monsoon trough. In contrast, the increased low-level relative vorticity over the western part of the WNP basin possibly plays a positive role in the increased TC counts over this region. The 600-hPa relative humidity increased significantly except for over the South China Sea (Fig. 5c). The decrease of TC counts over the WNP basin between the two sub-periods does not seem consistent with the moisture difference distribution, which is possibly due to there being enough mid-level moisture availability over the WNP basin for TC genesis during these two sub-periods. Consequently, changes in mid-level relative humidity appear to have little influence on changes in TC frequency.

4.2 Importance of change in WNP monsoon circulation on TCs associated with the monsoon-related LFPs

The WNP monsoon trough plays an important role in modulating TC activity over the WNP basin, as many previous studies have indicated (Wang and Zhou 2008; Wu et al. 2012; Wu and Wang 2015; Choi et al. 2016a,b; Wang and Wu 2016; Zhao et al. 2019a, b). As noted earlier, we find a significant correlation ($r = 0.51$) between TCs associated with the monsoon-related large-scale patterns and the total number TCs over the WNP basin. This section further explores changes in TCs associated with monsoon-associated large-scale patterns. WNP monsoon intensity (WNPMI) is computed following Wu et al. (2012), which is defined as 850-hPa relative vorticity averaged over 5° N–20° N, 120° E–180° E.

The correlation between the WNPMI and total TC counts over the WNP is statistically insignificant during both two sub-periods (Table 4), but an increase in the correlation is observed from −0.10 during 1979–1997 to 0.42 during 1998–2012. A significant increase in the inter-annual relationship between the WNPMI and the total number of TCs associated with monsoon-related flow patterns (SL, CR and GY) is also found. There is an insignificant correlation between TCs generated from monsoon-related flow patterns and the WNPMI during 1979–1997 ($r = 0.29$) and a significant correlation during 1998–2012 ($r = 0.83$). The inter-annual relationship between the WNPMI and TC cases associated with the SL pattern are significant during the whole period as well as during both sub-periods.

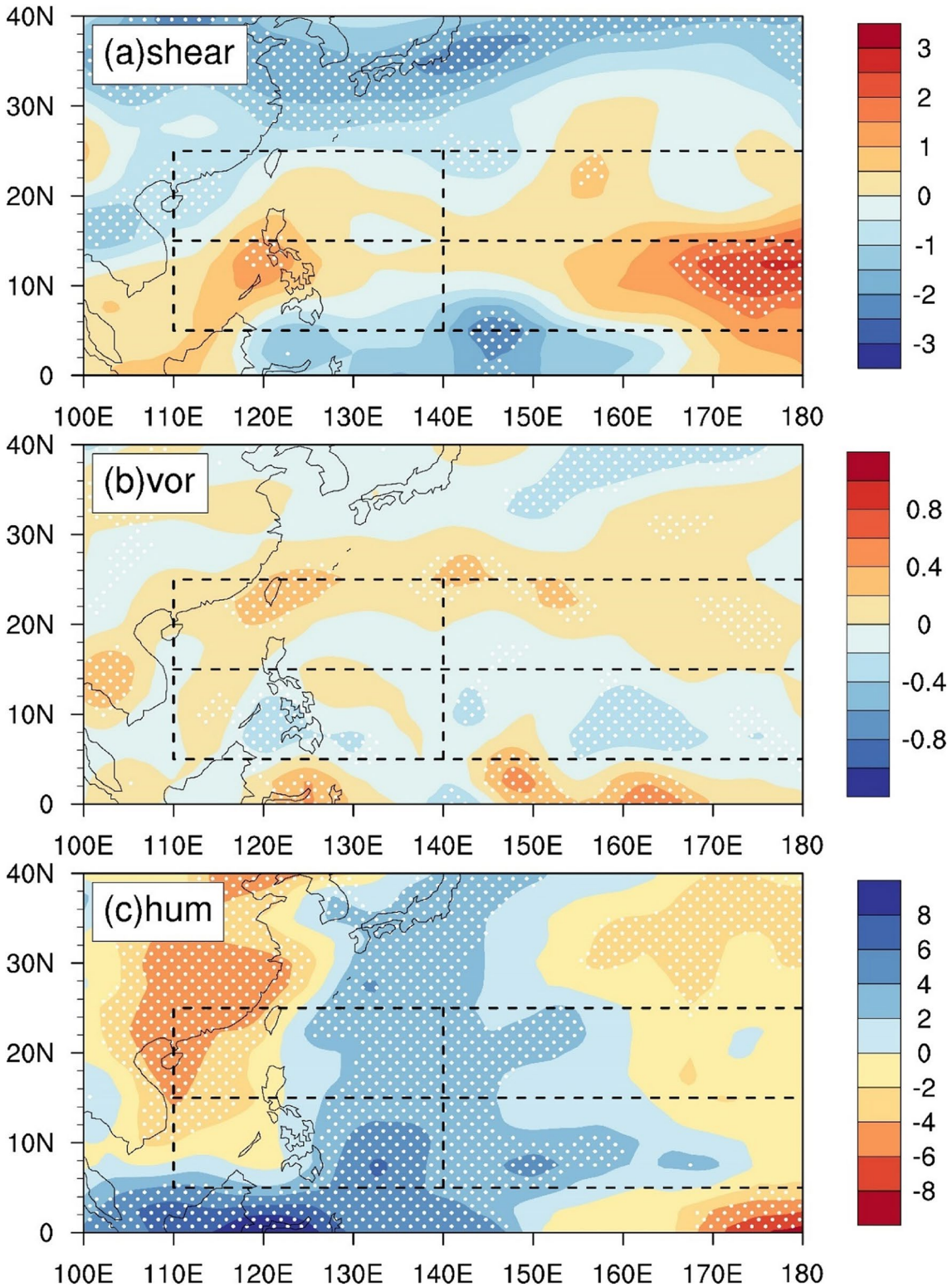

Fig. 5 Spatial distribution of the difference (1998–2012 minus 1979–1997) of average **a** vertical wind shear, **b** 850-hPa relative vorticity, and **c** 600-hPa relative humidity over May–October. The area with white dots indicates that the difference is significant at a 90% confidence level. The sub-regions are also show in figure: northwestern (110–140° E, 15–25° N), northeastern (140–180° E, 15–25° N), southwestern (110–140° E, 5–15° N), and southeastern region (140–180° E, 5–15° N)

Table 4 Correlation coefficients between the WNPMI and TC counts associated with the SL, CR, GY, EW, and PTC patterns, for the first sub-period: 1979–1997, the second sub-period: 1998–2012 and the whole period: 1979–2012

WNPMI	Total	SL + CR + GY	SL	CR	GY	EW	PTC
1979–2012	0.19	**0.47***	**0.43***	0.06	**0.40***	**−0.44***	−0.03
1979–1997	−0.10	0.29	**0.45***	−0.12	0.16	−0.23	−0.31
1998–2012	0.42	**0.83***	**0.69***	0.27	**0.62***	**−0.85***	−0.23

Correlations between WNPMI and TC counts associated with monsoon-related large-scale patterns (i.e., SL, CR and GY patterns) are also listed. The symbol "*" indicates that the correlation coefficients are significant at a 90% confidence level

Additionally, there is an inter-decadal change in the correlation between the WNPMI and TCs associated with the GY pattern, with a weak correlation ($r = 0.16$) from 1979–1997 but a significant correlation ($r = 0.62$) during 1998–2012. In contrast, there are insignificant correlations between the WNPMI and TCs associated with the CR pattern during both sub-periods (Table 4), partly weakening the linkage between the WNPMI and TCs associated with monsoon-related flow patterns. In summary, a significant correlation between the WNPMI and the total TCs over the WNP basin during 1998–2012 is primarily due to a significant correlation between the WNPMI and TCs associated with the SL and GY patterns. The correlation between the WNPMI and TCs associated with the EW pattern is found to be significant during 1998–2012 ($r = -0.85$), although there is no significant correlation between them during 1979–1997.

The dominance of strong cyclonic shear in the SL pattern can provide favorable low-level convergence conditions for TCG events (Harr and Chan 2005). Approximately 40% of TCG cases are found to be closely associated with the SL pattern. Figure 6a, b show the composite filed between years with high (> 1.0 STD: 1980, 1982, 1994, 1997, 2003, 2006) and low (< − 1.0 STD: 1986, 1995, 1998, 2001, 2010) TCs associated with the SL pattern. It shows a stronger monsoon circulation with stronger westerly wind and larger low-level relative vorticity. The vertical wind shear appears stronger over the southern WNP during years with more TCs associated with the SL pattern. These analyses suggest that TC genesis associated with the SL pattern depends mainly on the strength of the monsoon circulation, while the influence of vertical wind shear is relatively weak. During 1998–2012, the TCGs associated with the SL pattern significantly shift westward correspond to the weakening and westward shift of the monsoon trough. While, we also found an anomalous cyclonic circulation has prevailed north of the Philippines (Fig. 4), which possibly contributes to the increase of TCG counts over the northwestern WNP. The increase of TCGEs associated with the SL pattern over the western region offsets the decrease of TCGEs over the southeastern region, so there is no significant inter-decadal difference in the SL pattern.

Similar composites are shown between years with high (> 1.0 STD: 1979, 1989, 1991, 1993, 1994, 2000, 2001, 2002) and low (< − 1.0 STD: 1980, 1987, 1992, 1998, 2003, 2010) TCs associated with the CR pattern (Fig. 6c, d). As seen for the SL pattern, larger low-level relative vorticity over the WNP is found for years with more TCs associated with the CR pattern, although the low-level vorticity appears to be weaker than that during years with more TCs associated with the SL pattern. Significantly stronger westerly winds mainly appear near 15°N during years with more TCs associated with the CR pattern. Somewhat unexpectedly, the TC counts associated with the CR pattern correlate weakly with the WNPMI during the whole period as well as in each of the two sub-periods. This result is surprising given that the monsoon confluence region promotes the development of moist convection and is favorable for TCs associated with the CR pattern as pointed out by previous studies (Holland 1995; Ritchie and Holland 1999). Ritchie and Holland (1999) suggested that the formation of TCs associated with the CR pattern is mainly affected by the monsoon circulation and Pacific easterly waves. The result presented here, to a certain degree, indicates that TCs associated with the CR pattern are not only determined by the monsoon circulation. There may be nonlinear interactions between the monsoon circulation and tropical Pacific easterly waves.

The monsoon gyre is a synoptic-scale feature formed by the strong shear flow of the monsoon trough and disturbed by Pacific easterly waves with strong low-level vorticity conducive to TCG cases. The importance of Pacific easterly waves is reflected by a significant negative correlation ($r = -0.51$) between the TC counts associated with the GY and EW patterns (Table 3). Years with high (> 1.0 STD: 1981, 1984, 1987, 1993, 2003, 2004) and low (< − 1.0 STD:1983, 1992, 1995, 1996, 1998, 2000, 2005, 2007, 2008, 2010) TCs associated with the GY pattern were separately determined for each of the two sub-periods. A composite analysis between years with high and low TC counts associated with the GY pattern show stronger monsoon westerly winds and larger low-level relative vorticity during years with more TCs associated with the GY pattern (Fig. 6e, f), further stressing the importance of the monsoon trough and Pacific easterly waves. This result is consistent with the observation that

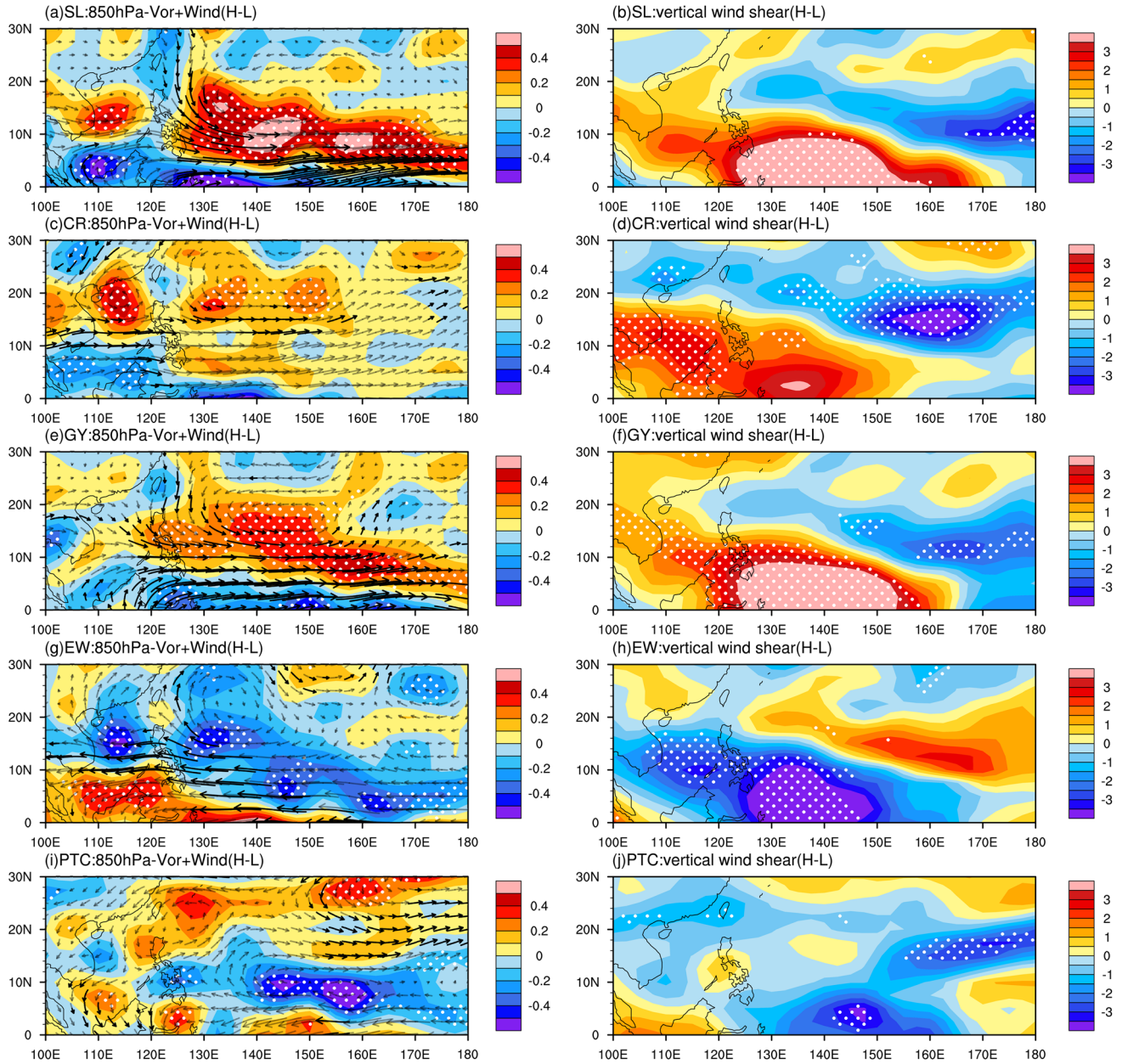

Fig. 6 Spatial distribution of the difference of composite May–October averaged anomaly of 850-hPa relative vorticity and wind, and vertical wind shear between high years and low years (High minus Low). The High (Low) years are identified separately for each of the two sub-periods by the standardized annual average frequency of TC associated with the SL (**a**, **b**), CR (**c**, **d**), GY (**e**, **f**), EW (**g**, **h**), and PTC (**i**, **j**) pattern larger (smaller) than 1.0 (− 1.0). The white dots and bold black vectors denote that the differences are significant at a 90% confidence level

most monsoon gyres are formed through the interaction of easterly waves with the monsoon trough as suggested by Chen et al. (2008). Associated with the westward shift of the monsoon trough and enhanced Pacific easterlies (Fig. 4), a significant decrease in TC cases associated with the GY pattern in the recent sub-period occurs, as would be expected.

4.3 Relationship between WNP TC distribution and SST

There has been a consensus on the greater importance of large-scale circulations on TCs over the WNP basin (Wang and Zhou 2008; Wu et al. 2012; Zong and Wu 2015a, b; Wu and Wang 2015; Wang and Wu 2016; Zhao et al. 2019a, b). One of the most important large-scale circulation systems

is the WNP monsoon circulation. The WNPMI has been shown in prior studies to be closely linked to ENSO on inter-annual time scales (Tanaka 1997; Wang et al. 2001; Vega et al. 2018). A significant correlation between the WNPMI and Niño-3.4 is also found here, with correlations of 0.81 during 1979–1997, of 0.89 during 1998–2012, and of 0.82 during 1979–2012. As suggested by previous studies noting the increased frequency of CP ENSO events during recent decades (Kao and Yu 2009; Cai et al. 2015; Wang 2019; Zhao and Wang 2019), there is an apparent inter-decadal change in the inter-annual relationship between the WNPMI and the EMI with a significant correlation of 0.44 during 1979–1997 and a more significant correlation of 0.80 during 1998–2012.

Correlation maps between TC counts associated with the SL pattern and global SST for the two sub-periods are shown in Fig. 8a, b. Areas with significant correlation are located over the tropical central Pacific during 1998–2012 but are not found in the previous sub-period 1979–1997. This is further confirmed by a weak correlation ($r=0.27$) and a significant correlation ($r=0.60$) between the EMI and TC counts associated with the SL pattern. Therefore, the significant association between the WNPMI and TCs associated with the SL pattern during the two sub-periods, and especially the increased association during the second sub-period, is likely closely related to the significant correlation between the WNPMI and Niño-3.4 as well as an increase in the correlation between the WNPMI and EMI. In response to the strengthened association between the WNPMI and EMI, the inter-annual relationship between the TCs associated with the GY pattern and the WNPMI becomes stronger during the second sub-period. During 1998–2012, the TCs associated with the GY pattern have a significant correlation of ($r=0.60/r=0.51$) with EMI/Niño-3.4, while their association is not significant ($r=0.04/r=0.27$) during 1979–1997. Similarly, the correlation between TCs associated with the EW pattern and EMI/Niño-3.4 is found to be significant during 1998–2012 ($r=-0.75/r=-0.74$) and non-significant during 1979–1997 ($r=0.07/r=-0.33$). Moreover, the large increase in the correlation between TCs associated with the EW pattern and WNPMI from −0.23 to 0.85 from 1979–1997 to 1998–2012, respectively, is also found to be related to the increase in the frequency of CP ENSO events (Table 4). These results are also confirmed by the CP ENSO-like correlation pattern during 1998–2012 (Fig. 7).

Changes in ENSO type during recent decades are closely related to the transition of the PDO phase (Kao and Yu 2009; Cai et al. 2015). In the late 1990s, the PDO changed from a warm phase to a cool phase. In addition to the strong association between ENSO and the

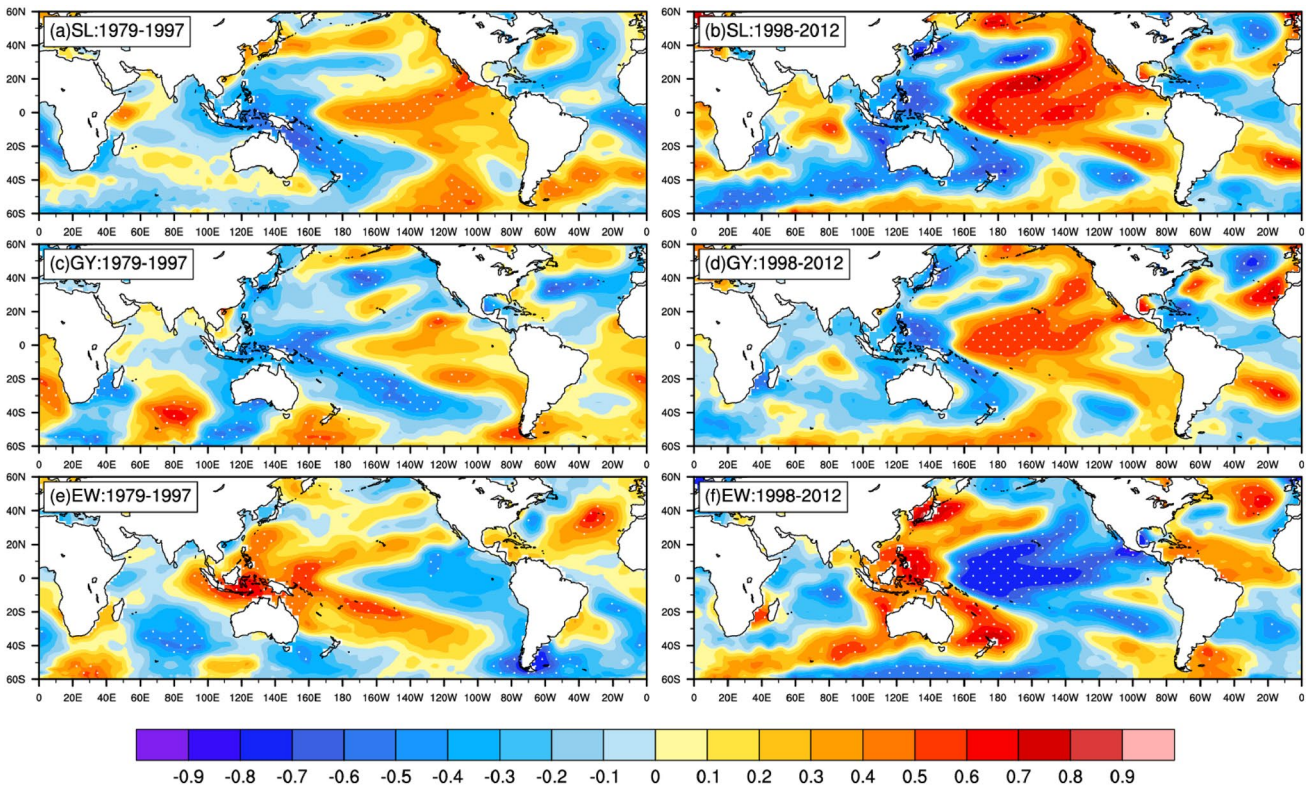

Fig. 7 Correlation patterns of TCs associated with the (**a**, **b**) SL pattern, (**c**, **d**) GY pattern and (**e**, **f**) EW pattern and SST during 1979–1997 and 1998–2012. White dots represent significant correlations at the 90% confidence level

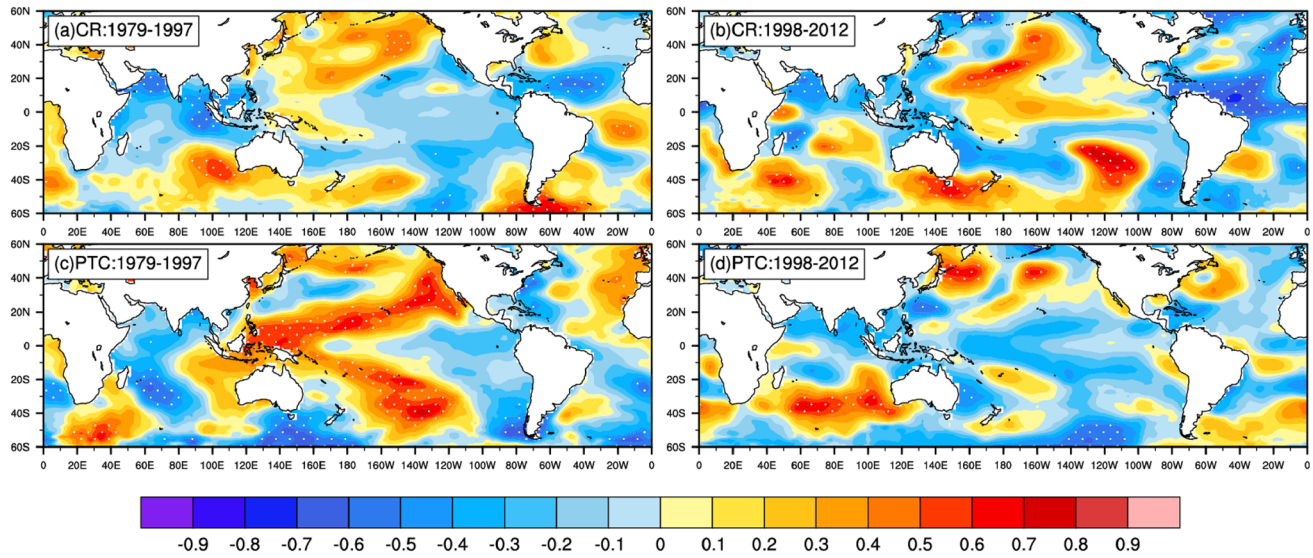

Fig. 8 As in Fig. 7, but with (**a**, **b**) corresponding to the CR pattern, and (**c**, **d**) to the PTC pattern

WNPMI, the PDO correlated insignificantly ($r = 0.06$) with the WNPMI during 1979–1997 which then became significant ($r = 0.62$) during 1998–2012. Correspondingly, the correlations between PDO and TCs associated with the SL/GY/ EW patterns are also insignificant ($r = -0.09/0.22/-0.07$) during 1979–1997 and become significant ($r = 0.62/0.45/-0.48$) during 1998–2012. Particularly, TCs associated with the CR pattern have non-significant correlation with tropical central-eastern Pacific during either sub-period (Fig. 8), but they do exhibit a significant correlation with SST over the tropical North Atlantic (TNA; 5.5° N–23.5° N, 15° W–57.5° W) during both sub-periods. An increased association during 1998–2012 is also observed between the TCs associated with the CR pattern and averaged SST over the TNA region, with a correlation of − 0.38 during 1979–1997 and − 0.64 during 1998–2012. The mechanism of how the TNA impacts TCs associated with the CR pattern deserves further study.

To investigate the associated physical mechanism driving changes of TCs associated with the PTC large-scale pattern over the WNP basin, the correlation maps between TC counts associated with the PTC large-scale pattern and global SST for the two sub-periods are shown in Fig. 8. Correlation patterns between TCs associated with PTC pattern and global SST have similarities to the PMM-like structure (Fig. 8c) during the period of 1979–1997, which is further confirmed by the significant correlation ($r = 0.41$) between TCs associated with PTC pattern and the PMM index (Zhang et al. 2016). In contrast, the PMM-like correlation pattern between them disappears during the second sub-period of 1998–2012. Correspondingly, a weak correlation ($r = 0.16$) between the PMM index and TCs associated with PTC pattern during 1998–2012 is found. The underlying physical mechanism on the PMM driving the TCs associated with the PTC pattern deserves further investigations.

4.4 Possible impact of recent enhanced Pacific easterly anomalies on TCs associated with the EW LFP

Until recently, the physical mechanism of how easterly waves develop directly into TCs remained unclear, although a strong association between them has been documented (Ritchie and Holland 1997; Chen et al. 2008). The associated physical mechanism on the interaction between easterly waves and the monsoon circulation (Chen et al. 2008) as well as the barotropic instability growth mechanism (Ritchie and Holland 1999) have been proposed. The difference in the composite environmental flow between years with high (> 1.0 STD: 1980, 1986, 1992, 1995, 1998, 2010) and low (< − 1.0 STD: 1979, 1982, 2002, 2006, 2009) TC counts associated with the EW pattern is opposite to that of the SL pattern (Fig. 6g, h), indicating a weakened monsoon circulation with strong easterly wind. However, the composite vertical wind shear shows weaker vertical wind shear over the southern of WNP during years with more TCs associated with the EW pattern, favoring TC genesis associated with the EW pattern in the easterly winds' environment. The strong association between TC frequency associated with the EW pattern and the monsoon circulation is reflected by a significant negative correlation between TC frequency associated with the EW pattern and TCs associated with the monsoon-related LFPs (i.e., SL, CR and GY patterns) for both sub-periods.

The correlation is − 0.70 during 1979–1997 and − 0.83 during 1998–2012. Together with the co-variability of the monsoon circulation over the WNP basin and tropical Pacific trade winds, the association between the WNPMI and TCs associated with the EW large-scale pattern during 1998–2012 becomes stronger in response to a strengthened Pacific easterly wave anomaly over the WNP basin.

Although a stronger association between the WNPMI and TCs associated with the EW large-scale pattern during 1998–2012 is observed, we find no significant difference of TCs associated with the EW large-scale pattern between the two sub-periods. This is possibly related to the changing impact of Rossby waves induced by TCs associated with the PTC large-scale pattern. According to the classification of TCs associated with the LFPs in Yoshida and Ishikawa (2013), the relatively minor PTC pattern has a large contribution to TCG when EW is the dominant pattern. They also noted that it also may be because the PTC pattern feeds vorticity into the easterly wave environment to trigger TCG cases. A change in the association between TCs associated with both the EW (major) and PTC (minor) patterns is found, with a significant correlation ($r = 0.44$) during 1979–1979 but an insignificant correlation ($r = 0.16$) during 1998–2012. During 1979–1997, the PTC has a stronger contribution to TCG associated with the EW pattern, possibly weakening the inter-annual relationship between TCs associated with the EW pattern and the WNPMI. In contrast, the propagation of Rossby wave energy dispersion to the southeast is hindered due to a significant decrease in the number of TCs associated with the PTC pattern as well as the resulting weakened contribution of PTC to TCG cases associated with the EW pattern. As expected, there is a decrease in the number of TCs associated with the EW pattern in the southeast region of the WNP basin and a stronger association between the WNPMI and TCs associated with the EW pattern.

4.5 Possible role of recent weakened easterly wind shear on TCs associated with the PTC LFP

As presented above, a substantial decrease in TC counts over the WNP basin is mainly due to a significant decrease in the number of TC counts associated with the PTC pattern during 1998–2012. The TCs associated with the PTC pattern prevail over the southeastern region of the WNP basin, where a significant decrease in the total TC counts is observed (Fig. 2f). Previous studies have suggested that the background wind field and moisture conditions are important for the development of TCs in Rossby wave trains (Li and Fu 2006; Li et al. 2006). As shown in Fig. 5, the weakening of vertical wind shear in the south-central WNP and the increase of relative humidity in the middle troposphere make the environment more conducive to the development of TCs during the second sub-period, partly countered by the observed weakening of 850-hPa relative vorticity. Figure 6i, j show the difference in the composite fields between years with high (> 1.0 STD:1992, 1995, 1996, 2000, 2004, 2012) and low (< − 1.0 STD: 1979, 1980, 1982, 1983, 2002, 2003, 2005) TCs associated with the PTC pattern. The patterns indicate a weakened monsoon circulation, but compared to the composite field of the EW pattern, there is also a weaker vertical wind shear near 17.5° N over the eastern of the WNP with stronger westerly wind. Figure 9 also shows that there is a strong easterly shear anomaly in this region. These promote the development of the low-level Rossby wave train and its southeastward propagation and thus, favor TC development associated with the PTC pattern accompanied with a weak vertical wind shear environment. Thus, there is weaker easterly shear in the later period between in the southeastern region of WNP (Fig. 10). During 1998–2012, this weaker easterly wind shear is partially driven by low-level anomalous easterlies and high-level anomalous westerlies over the southeastern portion of the WNP basin (Fig. 10), which would reduce the chance of TCs associated with the PTC large-scale pattern. This is similar to the results by Wang and Xie (1996) and Ge et al. (2007), who highlighted the effect of zonal wind shear on Rossby wave dispersion. They indicated that the generation of the barotropic Rossby mode under easterly wind shear could enhance the low-level wave amplitude, and acceleration of the low-level mean westerly flow could impact the energy dispersion to the southeast through the "Doppler shift effect". Figure 11 further shows the composite maps of environmental factors relative to the TC's center. It is clear that there is abnormal easterly wind shear north of the TC genesis location, further indicating that the easterly wind shear favors the propagation of the Rossby wave to the southeast and thus promotes TC genesis associated with the PTC pattern. In summary, the weaker easterly wind shear and the enhanced low-level easterlies are two important factors for changes of TCG counts associated with the PTC pattern.

The weaker easterly wind shear may also be closely linked to changes in the upper-level circulation. A clear westward shift of the TUTT is observed during 1998–2012 (Fig. 4), in agreement with previous studies (Wu et al. 2015; Zhao et al. 2019a). Further, the significant correlation ($r = -0.42$) between TC cases associated with the PTC pattern and TUTT during 1979–1997, becomes slightly weaker and non-significant ($r = -0.31$) during 1998–2012. Consistent with the extension and westward-shift of the TUTT during 1998–2012, anomalous upper-level westerly winds weaken the easterly wind shear and thus, the environment is not favorable for the development of Rossby waves and for TCG cases associated with the PTC pattern. During 1979–1997, more TCs associated with the PTC pattern possibly perturb the inter-annual relationship between the WNPMI and TCs

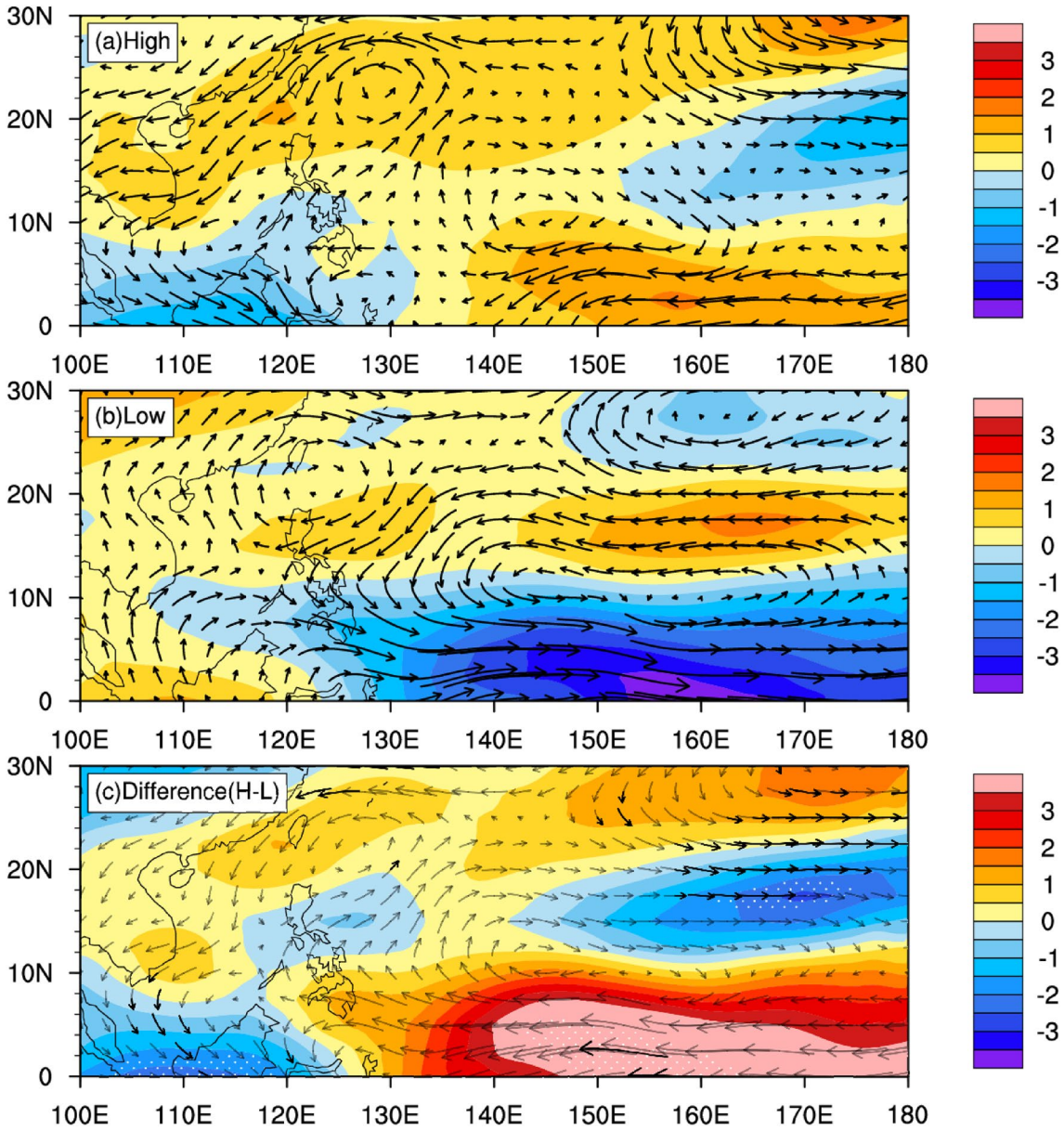

Fig. 9 Composite May–October averaged anomaly of 850-hPa wind (vectors) and zonal vertical wind shear between 200 and 850 hPa (shading) during **a** high years and **b** low years and **c** the difference between them (High-Low). The High (Low) years are identified separately during the two sub-periods by the standardized annual average frequency of TC associated with the PTC pattern larger (smaller) than 1.0 (− 1.0). The white dots and black vectors in **c** denote that the differences are significant at a 90% confidence level

associated with the SL, GY and EW patterns. In contrast, a significant decrease of TCs associated with the PTC pattern during 1998–2012 may weaken the influence of TCs associated with the PTC pattern to TCGs associated with other large-scale patterns.

5 Summary

This study focuses on the inter-decadal change in TCs associated with five basic large-scale patterns over the WNP basin during the boreal summer (May–October) between 1979–1997 (prior to the global warming hiatus) and 1998–2012 (during the global warming hiatus). All TCs associated with the five large-scale patterns over the WNP basin are identified by the objective classification method developed by Yoshida and Ishikawa (2013). There has been

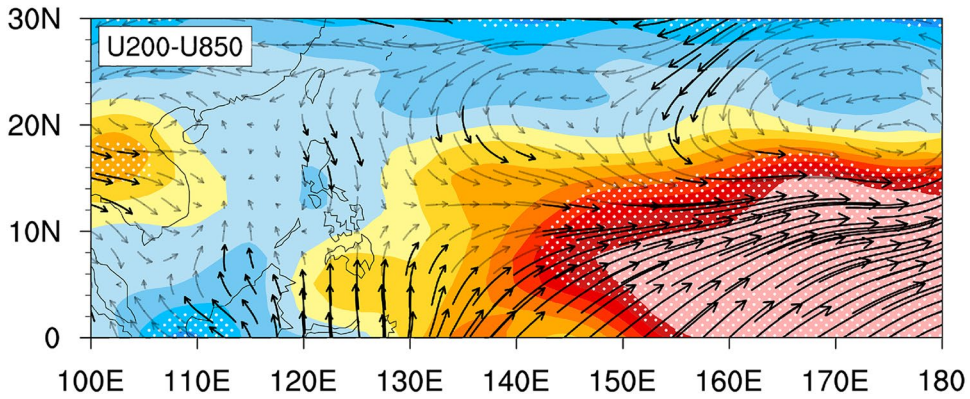

Fig. 10 Composite difference of 200-hPa wind (vector) and anomaly of zonal vertical wind shear (shading) over May–October between the two sub-periods (1998–2012 minus 1979–1997). The white dots and black vectors denote that the differences are significant at a 90% confidence level

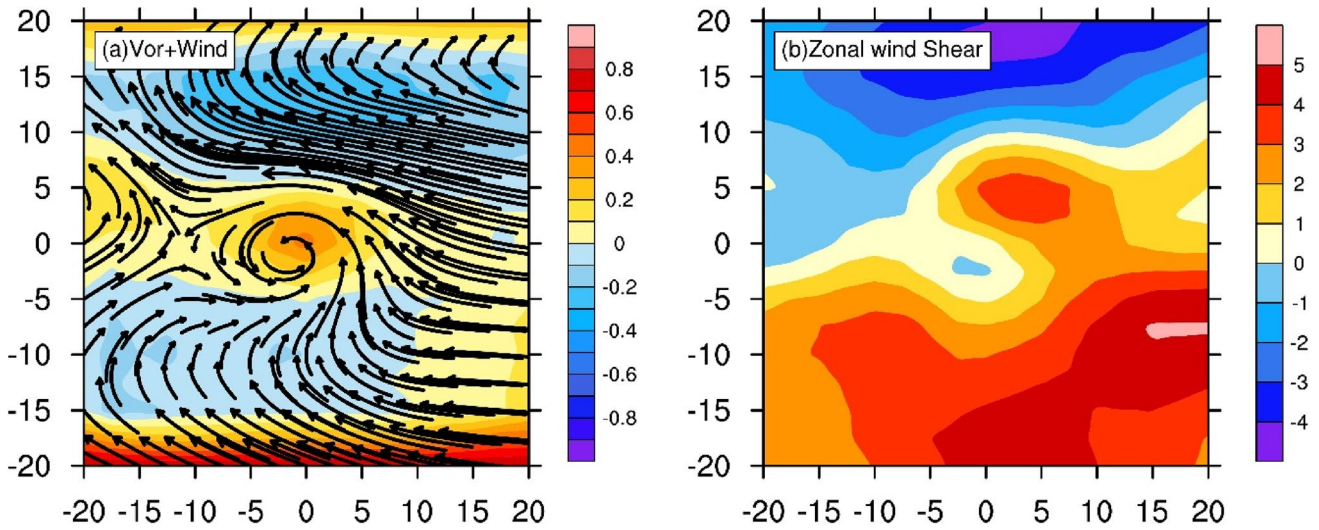

Fig.11 Composite averaged **a** 850-hPa wind (vectors) and 850-hPa relative vorticity (shading), and **b** zonal wind shear for total TCGEs associated with the PTC pattern on a coordinate system relative to the tropical cyclone center

a substantial decrease in TC counts over the WNP basin during 1998–2012, primarily due to a significant decrease in TCs associated with the PTC and GY patterns. The difference of TCs associated with the PTC pattern and GY pattern contribute ~ 66% and ~ 24% of the total difference of TCs between the two sub-periods. TC counts associated with the CR and EW patterns show a small decrease between the two sub-periods. Somewhat surprisingly, a weak increase of TCs associated with the SL pattern is found during 1998–2012.

Associated with a Mega-La Nina-like pattern, further research suggests that an increase of TCs associated with the SL pattern over the WNP basin is consistent with cyclonic shear located north of the Philippines during 1998–2012, seemingly counteracting the westward shift of the monsoon trough during the same period (Fig. 6i, j). Furthermore, the extension or retraction of the monsoon trough has a significant impact on the change of TC formation location but has little apparent influence on the total TC frequency associated with the SL pattern. A significant decrease in TCs associated with the GY pattern is possibly due to a weaker interaction of the monsoon circulation and Pacific easterly waves driven by the westward shift of the monsoon trough during the second sub-period. Weakened easterly wind shear appears to be important for the significant decrease in TCs associated with the PTC pattern during 1998–2012. No apparent change of TCs associated with the EW pattern is found between the two sub-periods, which may be due to the combined effect of both changes in tropical Pacific easterly anomalies and contributions from TCs associated with PTC pattern. During 1998–2012, enhanced tropical Pacific trade winds are beneficial for the westward propagation of easterly waves, resulting in more TCs associated with the EW pattern. This enhancement is largely offset by the reduced contribution of fewer TCs associated with the PTC pattern.

Changes in TCs associated with these five large-scale patterns are closely related to the changes in tropical SSTAs globally. TCs associated with the SL, GY, EW patterns are found to be closely linked to tropical central-eastern

Pacific SST, consistent with more CP ENSO events during 1998–2012 as suggested by previous studies (Kao and Yu 2009; Cai et al. 2015; Wang 2019; Zhao and Wang 2019). Meanwhile, a strengthened impact of tropical central-eastern Pacific SST on the WNP monsoon circulation has been observed since 1998 (Fig. 8), with a corresponding strengthened relationship between the WNP monsoon and TCs associated with the SL (GY/EW) pattern (Table 4). There are no significant interdecadal changes in TC frequency associated with the CR pattern between 1979–1997 and 1998–2012. There is also no significant connection between the WNP monsoon trough and the CR pattern, which may be related to the CR pattern being modulated by both the WNP monsoon and easterly waves. Surprisingly, changes in TCs associated with the CR pattern appear to be strongly associated with changes in TNA SSTAs, but the exact physical mechanism for how the TNA influences TCs associated with the CR pattern requires additional investigation. Lastly, TCs associated with the PTC pattern are not closely associated with more frequent CP ENSO events during 1998–2012 but do appear to be closely linked with the PMM during 1979–1997. Further studies of the response of TCs associated with the PTC pattern to climate regime shifts are needed.

Although previous studies suggested no apparent relationship between ENSO and the total TCs over the WNP basin (Lander 1994; Wang and Chan 2002; Camargo and Sobel 2005), TCs associated with the SL pattern over the WNP basin has a significant positive correlation with Nino-3.4 index (r = 0.46**). During the global warming hiatus period 1998–2012, a strengthening association between ENSO and both TCs associated with GY and EW patterns is found that is in partly due to a strengthening correlation between ENSO and WNP monsoon circulation compared to that during the accelerated warming epoch (1979–1997). When taking TCs associated the monsoon-related large-scale patterns including SL, GY and EW, there is a positive correlation between TCs associated with the three large-scale patterns and ENSO. In contrast, there is a significant negative correlation between ENSO and TCs associated with the EW pattern. To large extent, these results of this study would be helpful for prediction of TC activity at seasonal or long-time scales. Additionally, this study suggested a dominance of decrease of TCs associated with PTC pattern in the decreased of the total TCs over the WNP basin, the associated physical mechanism driving changes of TCs associated with the PTC pattern remains uncertain. Its enhanced understanding on changes of TCs associated with PTC pattern will further increase the predictability of TCs over the WNP basin.

As a final remark, this study also attempted to examine the role of environmental factors in the inter-decadal changes of TCs associated with five large-scale patterns using the genesis potential index (GPI) developed by Emanuel and Nolan (2004). This index has been used widely to assess the relative importance of large-scale factors in TC genesis at various time scales (Zhao et al. 2015, 2018; Wang and Moon 2017; Choi et al. 2019; Teng et al. 2019). Results show that the difference of GPI (global warming hiatus epoch minus accelerated warming epoch) shows a significant increase over the regions from 120° E to 160° E over the WNP, which appears to be contrary to observed difference of TCs between the two epochs (figure not shown). The observed differences between them show a significant decrease in TC counts over the WNP basin, which is especially due to a significant decrease of TCs over the southeastern part of WNP basin. In this sense, the GPI cannot represent well the inter-decadal change of TCs over the WNP basin and a better GPI index in reproducing the changes of TCs for all time scales is proposed in the future.

Acknowledgements We thank Prof. Hironori Fudeyasu from Yokohama National University in Japan for his valuable comments and suggestions in the revised stage of this manuscript. This research was jointly supported by the National Natural Science Foundation of China (Grant nos. 41675072, 41922033 and 41730961), the Natural Science Foundation of Jiangsu Province (Grant no. BK20181412), the QingLan Project of Jiangsu Province (R2017Q01), the project of the State Key Laboratory of Tropical Oceanography, South China Sea Institute of Oceanology, Chinese Academy of Science (no. LTO1904), Key Special Project for Introduced Talents Team of Southern Marine Science and Engineering Guangdong Laboratory (Guangzhou) (GML2019ZD0306), and the project of the "Six Talent Peaks Project" in Jiangsu Province (2019-JY-100). P. Klotzbach would like to acknowledge a grant from the G. Unger Vetlesen Foundation.

References

Ashok K, Behera SK, Rao SA et al (2007) El Niño Modoki and its possible teleconnection. J Geophys Res 112:C11007. https://doi.org/10.1029/2006JC003798

Bengtsson L, Hodges KI, Esch M et al (2007) How may tropical cyclones change in a warmer climate? Tellus Ser A Dyn Meteorol Oceanogr 59A:539–561. https://doi.org/10.1111/j.1600-0870.2007.00251.x

Cai W, Santoso A, Wang G et al (2015) ENSO and greenhouse warming. Nat Clim Change 5:849–859

Camargo SJ, Sobel AH (2005) Western North Pacific tropical cyclone intensity and ENSO. J Clim 18:2996–3006. https://doi.org/10.1175/JCLI3457.1

Chan JCL (2005) Interannual and interdecadal variations of tropical cyclone activity over the western North Pacific. Meteorol Atmos Phys 89:143–152. https://doi.org/10.1007/s00703-005-0126-y

Chan JCL (2008) Decadal variations of intense typhoon occurrence in the western North Pacific. Proc R Soc A Math Phys Eng Sci 464:249–272. https://doi.org/10.1098/rspa.2007.0183

Chen T-C, Wang S-Y, Yen M-C, Clark AJ (2008) Are tropical cyclones less effectively formed by easterly waves in the western North Pacific than in the North Atlantic? Mon Weather Rev 136:4527–4540. https://doi.org/10.1175/2008MWR2149.1

Choi J-W, Kim B-J, Zhang R et al (2016a) Possible relation of the western North Pacific monsoon to the tropical cyclone activity over western North Pacific. Int J Climatol 36:3334–3345. https://doi.org/10.1002/joc.4558

Choi KS, Kim HD, Kang SD, Shim CS (2016b) Decreasing trend of tropical cyclone genesis frequency in July-August over the western North Pacific in the last 20 years. Theor Appl Climatol 125:241–251. https://doi.org/10.1007/s00704-015-1497-8

Choi Y, Ha KJ, Jin FF (2019) Seasonality and El Niño diversity in the relationship between ENSO and western North Pacific tropical cyclone activity. J Clim 32:8021–8045. https://doi.org/10.1175/JCLI-D-18-0736.1

Choudhury D, Sen Gupta A, Sharma A et al (2017) Impacts of the tropical trans-basin variability on Australian rainfall. Clim Dyn 49:1617–1629. https://doi.org/10.1007/s00382-016-3405-z

Chu J-H, Sampson CR, Levine AS, Fukada E (2002) The joint typhoon warning center tropical cyclone best-tracks, 1945–2000. Ref NRL/MR/7540-02 16

Du Y, Yang L, Xie SP (2011) Tropical Indian Ocean influence on Northwest Pacific tropical cyclones in summer following strong El Niño. J Clim 24:315–322. https://doi.org/10.1175/2010JCLI3890.1

Emanuel K, Nolan DS (2004) Tropical cyclone activity and the global climate system. In: 26th conference on hurricanes and tropical meteorology, pp 240–241

Fyfe JC, Gillett NP, Zwiers FW (2013) Overestimated global warming over the past 20 years. Nat Clim Change 3:767–769. https://doi.org/10.1038/nclimate1972

Ge X, Li T, Zhou X (2007) Tropical cyclone energy dispersion under vertical shears. Geophys Res Lett 34:L23807. https://doi.org/10.1029/2007GL031867

Gray WM (1968) Global view of the origin of tropical disturbances and storms. Mon Weather Rev 96:669–700. https://doi.org/10.1175/1520-0493(1968)096<0669:GVOTOO>2.0.CO;2

Gray WM (1979) Hurricanes: their formation, structure and likely role in the tropical circulation. In: Shaw DB (ed) Meteorology over the tropical oceans. Royal Meteorological Society, James Glaisher House, Grenville Place, Bracknell, Berkshire, pp 155–218

Gray WM (1998) The formation of tropical cyclones. Meteorol Atmos Phys 67:37–69. https://doi.org/10.1007/BF01277501

Harr PA, Chan JCL (2005) Monsoon impacts on tropical cyclone variability. WMO Tech Doc 1266:512–542

He H, Yang J, Gong D et al (1990s) Decadal changes in tropical cyclone activity over the western North Pacific in the late 1990s. Clim Dyn 45:3317–3329. https://doi.org/10.1007/s00382-015-2541-1

Holland GJ (1995) Scale interaction in the Western Pacific Monsoon. Meteorol Atmos Phys 56:57–79. https://doi.org/10.1007/BF01022521

Hong C-C, Wu Y-K, Li T (1990s) Influence of climate regime shift on the interdecadal change in tropical cyclone activity over the Pacific Basin during the middle to late 1990s. Clim Dyn 47:2587–2600. https://doi.org/10.1007/s00382-016-2986-x

Hsu P-C, Chu P-S, Murakami H, Zhao X (2014) An abrupt decrease in the late-season typhoon activity over the Western North Pacific. J Clim 27:4296–4312. https://doi.org/10.1175/JCLI-D-13-00417.1

Hu Z-Z, Kumar A, Ren H-L et al (2013) Weakened interannual variability in the tropical Pacific Ocean since 2000. J Clim 26:2601–2613. https://doi.org/10.1175/JCLI-D-12-00265.1

Hu C, Zhang C, Yang S et al (2018) Perspective on the northwestward shift of autumn tropical cyclogenesis locations over the western North Pacific from shifting ENSO. Clim Dyn 51:2455–2465. https://doi.org/10.1007/s00382-017-4022-1

Huang B, Thorne PW, Banzon VF et al (2017) Extended reconstructed sea surface temperature, version 5 (ERSSTv5): upgrades, validations, and intercomparisons. J Clim 30:8179–8205. https://doi.org/10.1175/JCLI-D-16-0836.1

Jiang X, Zhao M, Waliser DE (2012) Modulation of tropical cyclones over the eastern Pacific by the intraseasonal variability simulated in an AGCM. J Clim 25:6524–6538. https://doi.org/10.1175/JCLI-D-11-00531.1

Kanamitsu M, Ebisuzaki W, Woollen J et al (2002) NCEP–DOE AMIP-II reanalysis (R-2). Bull Am Meteorol Soc 83:1631–1644. https://doi.org/10.1175/BAMS-83-11-1631

Kao H-Y, Yu J-Y (2009) Contrasting Eastern-Pacific and Central-Pacific types of ENSO. J Clim 22:615–632. https://doi.org/10.1175/2008JCLI2309.1

Kosaka Y, Xie SP (2013) Recent global-warming hiatus tied to equatorial Pacific surface cooling. Nature 501:403–407. https://doi.org/10.1038/nature12534

Knutson TR, McBride JL, Chan J et al (2010) Tropical cyclones and climate change. Nat Geosci 3:157–163. https://doi.org/10.1038/ngeo779

Kug JS, Jin FF, Il AS (2009) Two types of El Niño events: cold tongue El Niño and warm pool El Niño. J Clim 22:1499–1515. https://doi.org/10.1175/2008JCLI2624.1

Lander MA (1994) An exploratory analysis of the relationship between tropical storm formation in the western North Pacific and ENSO. Mon Weather Rev 122:636–651. https://doi.org/10.1175/1520-0493(1994)122<0636:AEAOTR>2.0.CO;2

Lee T, McPhaden MJ (2010) Increasing intensity of El Niño in the central-equatorial Pacific. Geophys Res Lett. https://doi.org/10.1029/2010GL044007

Lee C-S, Cheung KKW, Hui JSN, Elsberry RL (2008) Mesoscale features associated with tropical cyclone formations in the Western North Pacific. Mon Weather Rev 136:2006–2022. https://doi.org/10.1175/2007MWR2267.1

Li T, Fu B (2006) Tropical cyclogenesis associated with Rossby wave energy dispersion of a preexisting typhoon. Part I: satellite data analyses. J Atmos Sci 63:1377–1389. https://doi.org/10.1175/JAS3692.1

Li T, Ge X, Wang B, Zhu Y (2006) Tropical cyclogenesis associated with Rossby wave energy dispersion of a preexisting typhoon. Part II: numerical simulations. J Atmos Sci 63:1390–1409. https://doi.org/10.1175/JAS3693.1

Lin I-I, Chan JCL (2015) Recent decrease in typhoon destructive potential and global warming implications. Nat Commun 6:7182. https://doi.org/10.1038/ncomms8182

Liu KS, Chan JCL (2008) Interdecadal variability of western North Pacific tropical cyclone tracks. J Clim 21:4464–4476. https://doi.org/10.1175/2008JCLI2207.1

Liu KS, Chan JCL (2013) Inactive period of western north pacific tropical cyclone activity in 1998–2011. J Clim 26:2614–2630. https://doi.org/10.1175/JCLI-D-12-00053.1

Matsuura T, Yumoto M, Iizuka S (2003) A mechanism of interdecadal variability of tropical cyclone activity over the western North Pacific. Clim Dyn 21:105–117. https://doi.org/10.1007/s00382-003-0327-3

Maue RN (2011) Recent historically low global tropical cyclone activity. Geophys Res Lett 38:L14803. https://doi.org/10.1029/2011GL047711

McBride JL, Zehr R (1981) Observational analysis of tropical cyclone formation. Part II: comparison of non-developing versus developing systems. J Atmos Sci 38:1132–1151. https://doi.org/10.1175/1520-0469(1981)038<1132:OAOTCF>2.0.CO;2

Molinari J, Vollaro D (2013) What percentage of Western North pacific tropical cyclones form within the monsoon trough? Mon Weather Rev 141:499–505. https://doi.org/10.1175/MWR-D-12-00165.1

Onogi K, Tsutsui J, Koide H et al (2007) The JRA-25 Reanalysis. J Meteorol Soc Jpn Ser II 85:369–432. https://doi.org/10.2151/jmsj.85.369

Oouchi K, Yoshimura J, Yoshimura H et al (2006) Tropical cyclone climatology in a global-warming climate as simulated in a 20 km-mesh global atmospheric model: frequency and wind intensity analyses. J Meteorol Soc Jpn Ser II 84:259–276. https://doi.org/10.2151/jmsj.84.259

Ritchie EA, Holland GJ (1999) Large-scale patterns associated with tropical cyclogenesis in the Western Pacific. Mon Weather Rev 127:2027–2043. https://doi.org/10.1175/1520-0493(1999)127<2027:LSPAWT>2.0.CO;2

Schreck CJ, Knapp KR, Kossin JP (2014) The impact of best track discrepancies on global tropical cyclone climatologies using IBTrACS. Mon Weather Rev 142:3881–3899. https://doi.org/10.1175/MWR-D-14-00021.1

Tanaka M (1997) Interannual and Interdecadal Variations of the Western North Pacific Monsoon and Baiu Rainfall and their relationship to the ENSO Cycles. J Meteorol Soc Jpn Ser II 75:1109–1123. https://doi.org/10.2151/jmsj1965.75.6_1109

Teng HF, Lee CS, Hsu HH et al (2019) Tropical cloud cluster environments and their importance for tropical cyclone formation. J Clim 32:4069–4088. https://doi.org/10.1175/JCLI-D-18-0679.1

Tollefson J (2014) Climate change: the case of the missing heat. Nature 505:276–278. https://doi.org/10.1038/505276a

Vega I, Gallego D, Ribera P et al (2018) Reconstructing the Western North Pacific summer monsoon since the late nineteenth century. J Clim 31:355–368. https://doi.org/10.1175/JCLI-D-17-0336.1

Verdon DC, Franks SW (2006) Long-term behaviour of ENSO: interactions with the PDO over the past 400 years inferred from paleoclimate records. Geophys Res Lett 33:L06712. https://doi.org/10.1029/2005GL025052

Wang C (2019) Three-ocean interactions and climate variability: a review and perspective. Clim Dyn 53:5119–5136. https://doi.org/10.1007/s00382-019-04930-x

Wang B, Chan JCL (2002) How strong ENSO events affect tropical storm activity over the Western North Pacific*. J Clim 15:1643–1658. https://doi.org/10.1175/1520-0442(2002)015<1643:HSEEAT>2.0.CO;2

Wang C, Wu L (2015) Influence of future tropical cyclone track changes on their basin-wide intensity over the western North Pacific: downscaled CMIP5 projections. Adv Atmos Sci 32:613–623. https://doi.org/10.1007/s00376-014-4105-4

Wang C, Wu L (2016) Interannual shift of the tropical upper-tropospheric trough and its influence on tropical cyclone formation over the western North Pacific. J Clim 29:4203–4211. https://doi.org/10.1175/JCLI-D-15-0653.1

Wang B, Xie X (1996) Low-frequency equatorial waves in vertically sheared zonal flow. Part I: stable waves. J Atmos Sci 53:449–467. https://doi.org/10.1175/1520-0469(1996)053<0449:LFEWIV>2.0.CO;2

Wang B, Zhou X (2008) Climate variation and prediction of rapid intensification in tropical cyclones in the western North Pacific. Meteorol Atmos Phys 99:1–16. https://doi.org/10.1007/s00703-006-0238-z

Wang B, Wu R, Lau K-M (2001) Interannual variability of the Asian summer monsoon: contrasts between the Indian and the Western North Pacific-East Asian Monsoons*. J Clim 14:4073–4090. https://doi.org/10.1175/1520-0442(2001)014<4073:IVOTAS>2.0.CO;2

Wang C, Wang B, Wu L (2019) A region-dependent seasonal forecasting framework for tropical cyclone genesis frequency in the western North Pacific. J Clim 32:8415–8435. https://doi.org/10.1175/JCLI-D-19-0006.1

Wu L, Wang B (2004) Assessing impacts of global warming on tropical cyclone tracks*. J Clim 17:1686–1698. https://doi.org/10.1175/1520-0442(2004)017<1686:AIOGWO>2.0.CO;2

Wu L, Wang C (1970s) Has the western pacific subtropical high extended westward since the late 1970s? J Clim 28:5406–5413. https://doi.org/10.1175/JCLI-D-14-00618.1

Wu L, Wen Z, Huang R, Wu R (2012) Possible linkage between the monsoon trough variability and the tropical cyclone activity over the Western North Pacific. Mon Weather Rev 140:140–150. https://doi.org/10.1175/MWR-D-11-00078.1

Wu L, Wang C, Wang B (2015) Westward shift of western North Pacific tropical cyclogenesis. Geophys Res Lett 42:1537–1542. https://doi.org/10.1002/2015GL063450

Yokoi S, Takayabu YN (2013) Attribution of decadal variability in tropical cyclone passage frequency over the Western North Pacific: a new approach emphasizing the genesis location of cyclones. J Clim 26:973–987. https://doi.org/10.1175/JCLI-D-12-00060.1

Yoshida R, Ishikawa H (2013) Environmental factors contributing to tropical cyclone genesis over the Western North Pacific. Mon Weather Rev 141:451–467. https://doi.org/10.1175/MWR-D-11-00309.1

Yu JY, Kao HY (2007) Decadal changes of ENSO persistence barrier in SST and ocean heat content indices: 1958–2001. J Geophys Res Atmos. https://doi.org/10.1029/2006JD007654

Yu J-Y, Kao H-Y, Lee T, Kim ST (2011) Subsurface ocean temperature indices for Central-Pacific and Eastern-Pacific types of El Niño and La Niña events. Theor Appl Climatol 103:337–344. https://doi.org/10.1007/s00704-010-0307-6

Yu J-Y, Kao P, Paek H et al (2015) Linking emergence of the Central Pacific El Niño to the Atlantic Multidecadal oscillation. J Clim 28:651–662. https://doi.org/10.1175/JCLI-D-14-00347.1

Yumoto M, Matsuura T (2001) Interdecadal variability of tropical cyclone activity in the Western North Pacific. J Meteorol Soc Jpn 79:23–35. https://doi.org/10.2151/jmsj.79.23

Zehr RM (1992) Tropical Cyclogenesis in the Western North Pacific. NOAA technical report NESDIS 61

Zhang Q, Wu L, Liu Q (2009) Tropical cyclone damages in China 1983–2006. Bull Am Meteorol Soc 90:489–496. https://doi.org/10.1175/2008BAMS2631.1

Zhang Q, Zhang W, Chen YD, Jiang T (2011) Flood, drought and typhoon disasters during the last half-century in the Guangdong province, China. Nat Hazards 57:267–278. https://doi.org/10.1007/s11069-010-9611-9

Zhang W, Leung Y, Fraedrich K (2015) Different El Niño types and intense typhoons in the Western North Pacific. Clim Dyn 44:2965–2977. https://doi.org/10.1007/s00382-014-2446-4

Zhang W, Vecchi GA, Murakami H et al (2016) The Pacific meridional mode and the occurrence of tropical cyclones in the Western North Pacific. J Clim 29:381–398. https://doi.org/10.1175/JCLI-D-15-0282.1

Zhao H, Wang C (2016) Interdecadal modulation on the relationship between ENSO and typhoon activity during the late season in the western North Pacific. Clim Dyn 47:315–328. https://doi.org/10.1007/s00382-015-2837-1

Zhao H, Wang C (2019) On the relationship between ENSO and tropical cyclones in the western North Pacific during the boreal summer. Clim Dyn 52:275–288. https://doi.org/10.1007/s00382-018-4136-0

Zhao H, Wu L, Zhou W (2010) Assessing the influence of the ENSO on tropical cyclone prevailing tracks in the western North Pacific. Adv Atmos Sci 27:1361–1371. https://doi.org/10.1007/s00376-010-9161-9

Zhao H, Yoshida R, Raga GB (2015) Impact of the Madden–Julian oscillation on Western North Pacific tropical cyclogenesis associated with large-scale patterns. J Appl Meteorol Climatol 54:1413–1429. https://doi.org/10.1175/JAMC-D-14-0254.1

Zhao H, Wang C, Yoshida R (2016) Modulation of tropical cyclogenesis in the western North Pacific by the quasi-biweekly oscillation.

Adv Atmos Sci 33:1361–1375. https://doi.org/10.1007/s00376-016-5267-z

Zhao H, Duan X, Raga GB, Klotzbach PJ (2018) Changes in characteristics of rapidly intensifying western North Pacific tropical cyclones related to climate regime shifts. J Clim 31:8163–8179. https://doi.org/10.1175/JCLI-D-18-0029.1

Zhao H, Chen S, Klotzbach PJ (2019a) Recent strengthening of the relationship between the western North Pacific monsoon and western North Pacific tropical cyclone activity during the boreal summer. J Clim 32:8283–8299. https://doi.org/10.1175/JCLI-D-19-0016.1

Zhao H, Chen S, Raga GB et al (2019b) Recent decrease in genesis productivity of tropical cloud clusters over the Western North Pacific. Clim Dyn 52:5819–5831. https://doi.org/10.1007/s00382-018-4477-8

Zong H, Wu L (2015a) Re-examination of tropical cyclone formation in monsoon troughs over the western North Pacific. Adv Atmos Sci 32:924–934. https://doi.org/10.1007/s00376-014-4115-2

Zong H, Wu L (2015b) Synoptic-scale influences on tropical cyclone formation within the Western North Pacific monsoon trough. Mon Weather Rev 143:3421–3433. https://doi.org/10.1175/MWR-D-14-00321.1

Affiliations

Kai Zhao[1] · Haikun Zhao[2,3] · Graciela B. Raga[4] · Ryuji Yoshida[5,6,7,8] · Weiqiang Wang[3,9,10] · Philip J. Klotzbach[11]

1 Key Laboratory of Meteorological Disaster, Ministry of Education (KLME), Nanjing University of Information Science and Technology, Nanjing, China

2 Key Laboratory of Meteorological Disaster, Ministry of Education (KLME), Joint International Research Laboratory of Climate and Environment Change (ILCEC), Collaborative Innovation Center on Forecast and Evaluation of Meteorological Disaster (CIC-FEMD), Pacific Typhoon Research Center, Earth System Modeling Center, Nanjing University of Information Science and Technology, Nanjing 210044, China

3 State Key Laboratory of Tropical Oceanography, South China Sea Institute of Oceanology, Chinese Academy of Sciences, Guangzhou, China

4 Centro de Ciencias de la Atmósfera, Universidad Nacional Autónoma de Mexico, Mexico City, Mexico

5 CIRES, University of Colorado Boulder, Boulder, CO, USA

6 NOAA Earth System Research Laboratory, Boulder, CO, USA

7 RIKEN Center for Computational Science, Kobe, Japan

8 Research Center for Urban Safety and Security, Kobe University, Kobe, Japan

9 Southern Marine Science and Engineering Guangdong Laboratory (Guangzhou), Guangzhou, China

10 Innovation Academy of South China Sea Ecology and Environmental Engineering, Chinese Academy of Sciences, Guangzhou, China

11 Department of Atmospheric Science, Colorado State University, Fort Collins, CO, USA